The effect of variable transmissions on photometric redshifts

Jean Coupon[1] (University of Geneva) et al.

February 11, 2018

1 Abstract

The variation of the photometric transmissions affect the computation of photo-z's and the color selection of cluster-z's. The biggest impact of variable transmissions on photo-z's is a shift in mean redshift for an ensemble of galaxies (as per tomographic bin), mainly caused by a shift or a skewing of the transmission (from manufacturing or incidence angle). A shift as small as 10 Angstroms (1 nm) creates a bias on an ensemble of galaxies which is on the same order of magnitude as the requirement on the mean redshift estimate ($\Delta z = 0.002(1+z)$) per tomographic bin and therefore cannot be ignored in the photo-z processing for cosmic shear analysis. For an individual galaxy the effect will be small (excluding the rare cases where a strong emission line lies at the edge of the filter), so that the performances on scatter and oultier rate will be hardly affected. For instance one must pay a particular attention at the variations occuring on scales where the shear-shear 2-point correlation is measured (typically a few arcmin scale), and where a variation in mean redshift will artifically boost the amplitude of the power spectrum on those scales.

2 Introduction

This document aims to address the impact of variable photometric transmissions on Euclid photometric redshifts (hereafter photo-z's). In each tomographic bin, the mean redshift of the ensemble of galaxies used for cosmic shear must be known to very high accuracy and is highly sensitive to systematics in color space. So the most problematic impact from transmissions with variable responses is expected to be a scale-dependent systematic error on the mean redshift, i.e. the *unknown* difference between the measured and true mean redshift per tomographic bin (the known difference, the "bias", being calibrated with spectroscopic redshifts and not expected to vary as a function of position in the sky). Variable transmissons will also affect the scatter (and to a lesser extent the number of catastrophic errors) but we assume that the mean redshift issue will largely dominate over the others and therefore we restrict ourselves to quantify the shift on the mean redshift only.

To quantify the effect, we use real galaxies from COSMOS with emulated fluxes. To measure the shift in mean redshift, we first emulate the fluxes and compute the photo-z's assuming reference (fixed) transmissions in both steps. Then, we vary the transmissions to emulate new fluxes, and we compute again photo-z's with the reference transmissions.

The approach we take in this study is to model a range of typical variations, based on input from various people reporting the behaviour of different instruments, and to estimate the corresponding impact on photo-z accuracy. Therefore, this document must serve as a reference for evaluating the impact *when the exact variations are known*, which will depend on the exact instrument and observing conditions of ground-based data used for Euclid. We stress that this document is *not* the actual prediction of systematics in mean redshift that will exist in the Euclid survey.

3 Problem

The photo-z requirements for Euclid fall into two broad categories: 1) photo-z precision and 2) mean redshift accuracy. The former translates into the traditionally quoted scatter and catastrophic failure (or outlier rate) estimates. Those have been revised by the Euclid science ground segement to be expressed as probability distribution functions (PDF) but, on point estimates, would be equivalent to a scatter smaller than $0.05 \times (1+z)$ and an outlier rate smaller than 10% for galaxies used in the cosmic shear probe. The main leverage to increase the precision is to improve the photometry signal-to-noise ratio (SNR) per source and

[1]Contact: jean.coupon@unige.ch

photo-z algorithms (we confirmed within OU-PHZ that a combination of template fitting and machine learning is the best tool to achieve the precision goals).

The specification on accuracy is that, per tomographic bin (there will be 10 bins between $0.2 < z < 2.0$), the mean redshift of the ensemble must be known with better accuracy than $\Delta z = 0.002 \times (1 + z)$. The current baseline of OU-PHZ is to use spectroscopic redshifts (hereafter spec-z's), matched in color to the Euclid galaxies, to correct for the residual redshift bias. The validation of this procedure will be done with clustering redshifts (hereafter cluster-z).

Hence the Euclid galaxies must be observed with stable transmissions, identical to that of the galaxies with spec-z's used for the mean redshift calibration. The problem we address here is when Euclid galaxies are observed in different transmissions compared to the spec-z sample. What is the impact on the mean redshift and from what point do we fail to meet the accuracy requirement, given a type and strength of variation?

4 Theory

4.1 Definition of a variable transmission

A "photometric transmission" is everything between the source and the detector. It includes (starting from the source itself) the inter-galtic medium (IGM), the Milky Way extinction, the atmosphere (for ground-based facilities), the instrument sensitivity, the photometric filter and the quantum efficiency of the detector. In most cases, the Milky Way extinction and the photometric filter will be the main source of variations. In this study our main focus is on the filter variations. So in the rest of the document, "transmission" means filter response.

4.2 Impact on photo-z's

The photometric redshift method is a way to predict a galaxy redshift PDF from a set of colors and brightness (or simply fluxes - the difference between the two set of quantities being in the way to optimise the photometry measurement). In principle any photo-z method makes use of all the color information but the most informative pieces of information is when the galaxy SED strongest features are moving through the filters.

The most prominent features are the Lyman ($\sim$ 1000 Angstroms) and Balmer ($\sim$ 4000 Angstroms) breaks. The Euclid-survey filter set is optimised to properly constrain the Balmer break in the range $0.2 < z < 2.0$ with a filter set going from 3000 to 10000 Angstroms (*ugrizYJH* and *vis* filters).

In the forthcoming sections, we will quantify the exact impact but, to first order, the main impact on photo-z's is when the Balmer break at a given redshift enters a filter whose transmission varies (this is what we will focus on). As an example, a galaxy will have its Balmer break enter the *r*-band at $z \sim 0.6$:

$$z = \frac{\lambda_{\text{mesured}}}{\lambda_{\text{emitted}}} - 1 = \frac{6400}{4000} - 1 = 0.6 \tag{1}$$

So, a transmission shift ΔA in the *r*-band translates into a redshift difference at $z \sim 0.6$ of:

$$\Delta z = \frac{\Delta\lambda(A)}{4000} \tag{2}$$

$$\Delta z_{\text{req}} < 0.002 \times (1 + z) = \frac{\Delta\lambda(A)}{4000} \tag{3}$$

so

$$\Delta\lambda(A) < 0.002 \times (1 + z) \times 4000 \tag{4}$$

Neglecting the contribution from the other bands, the requirement on the mean redshift accuracy, $0.002 \times (1 + z)$, would translate into a transmission shift of $0.002 \times 1.6 \times 4000 = 13$ Angstrom (1.3 nm). This means that any galaxy observed with a *r*-band affected by a shift larger than 12 Angstroms but calibrated with spec-z's observed with the reference *r*-band filter must be corrected from the variation of the transmission to meet the mean redshift accuracy requirement.

4.3 Measured variations on current filters

We summarise here the variations measured on current instruments, passed by various people involved in these projects and from the literature. It does not necessarily match what will be encountered in the Euclid survey but it gives an overview of the types and typical ranges of the filter transmission variations seen nowadays.

4.3.1 Adopted metric

We characterise the filter variations through the first moments of the transmission curve: the mean, the standard deviation and the skewness. The first two moments describes the shift and widening (or shrinking) of the filter, whereas the skewness is a measurement of the asymetry of the filter. We compare the three quantities to that of a reference filter (in the measurement of the real filter we take the values measured at the center), in Angstroms (ΔA). All three quantities are correlated with each other, so that if, for example, only the cut-off of a filter (and not the cut-on) is varying, both the mean and standard deviations will vary simulatenously. Similarly, if the skewness is varying, the mean will vary as well. As the effect is small, we show the skewness times 100 (in fact the higher impact of the asymetry will be a change in effective mean wavelength).

In principle the higher-order moments will describe the filter variations in greater details, but we beleive the above three will dominate over the others and are simple quantities to tie together real-life and simulated filters.

4.3.2 OmegaCam at VST

These are measured transmissions as a function of position on the focal plane of the *ugriz* OmegaCam filters received from Konrad Kuijken. They include both the manufacturing variations as a function of position and the incidence angle. We take the *r*-band filter as an example.

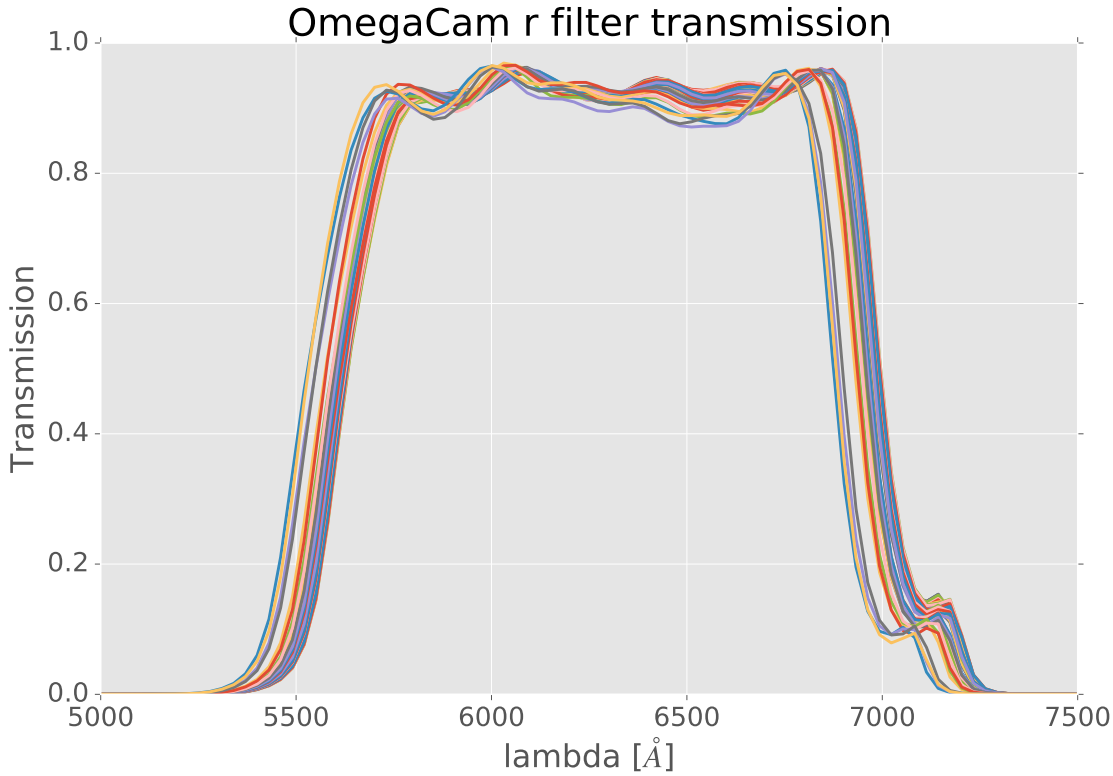

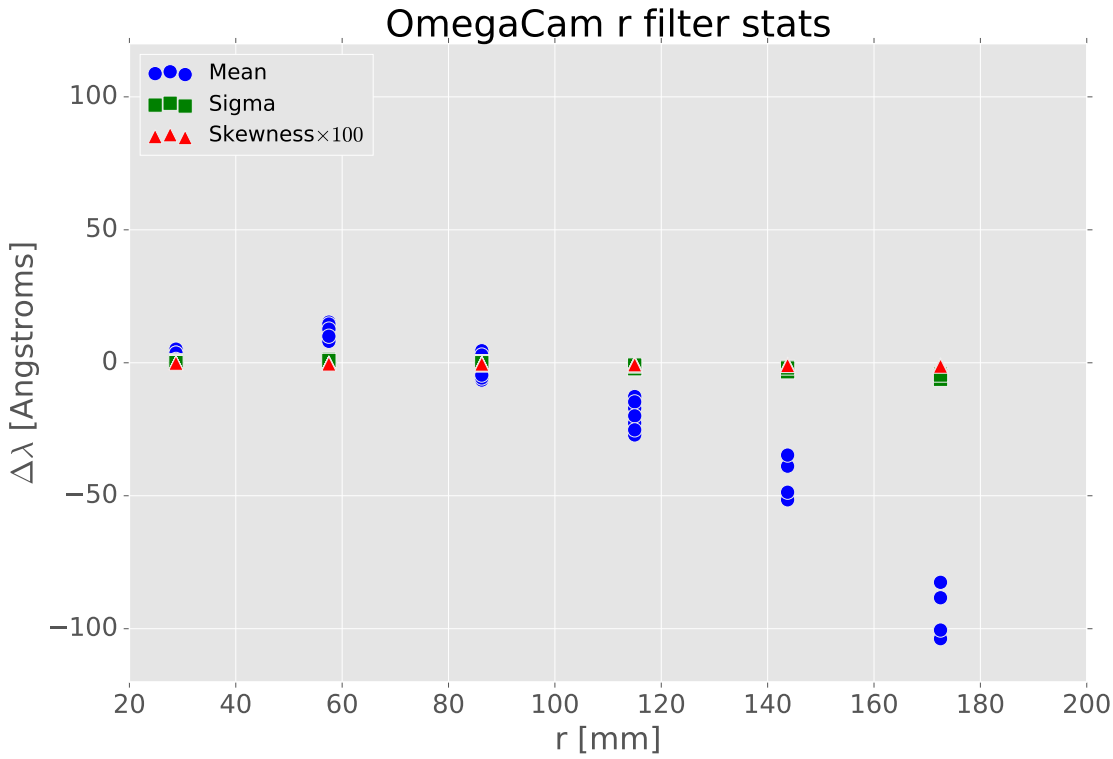

4.3.3 JAST at Javalembre

The Javalambre Auxiliary Survey Telescope (JAST/T80) is the companion telescope of the Javalambre Survey Telescope. The filter transmissions for the g-band filter as a function of position on the focal plane were given by Jesus Varela. They only include the manufacturing variations and not the incidence angle (to check).

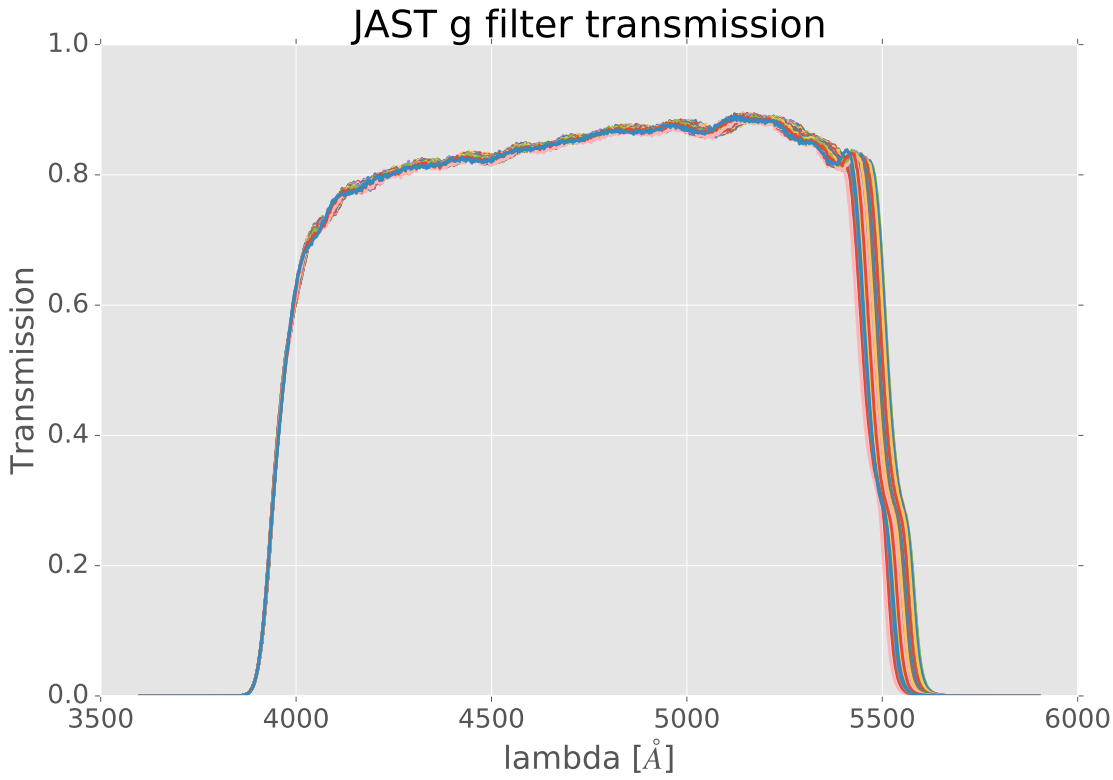
JAST g filter transmission
Transmission
lambda [Å]
1.0
0.8
0.6
0.4
0.2
0.0
3500
4000
4500
5000
5500
6000

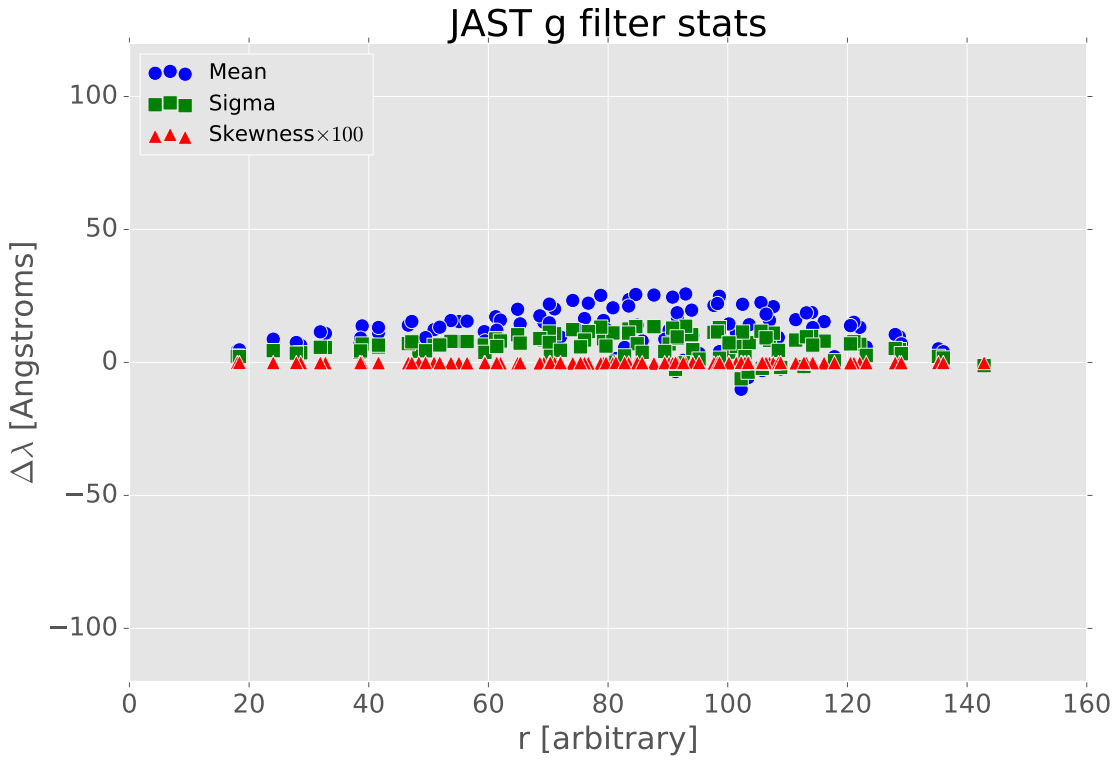
JAST g filter stats
Mean
Sigma
Skewness×100
Δλ [Angstroms]
r [arbitrary]
100
50
0
−50
−100
0
20
40
60
80
100
120
140
160

4.3.4 MegaCam at CFHT

Measurements based on standard stars exist for the old MegaCam filters from Betoule et al. (2013). We show below the *r*-band measurements at several radii from the filter center. These varations include everything as they are measured on standard stars in real conditions.

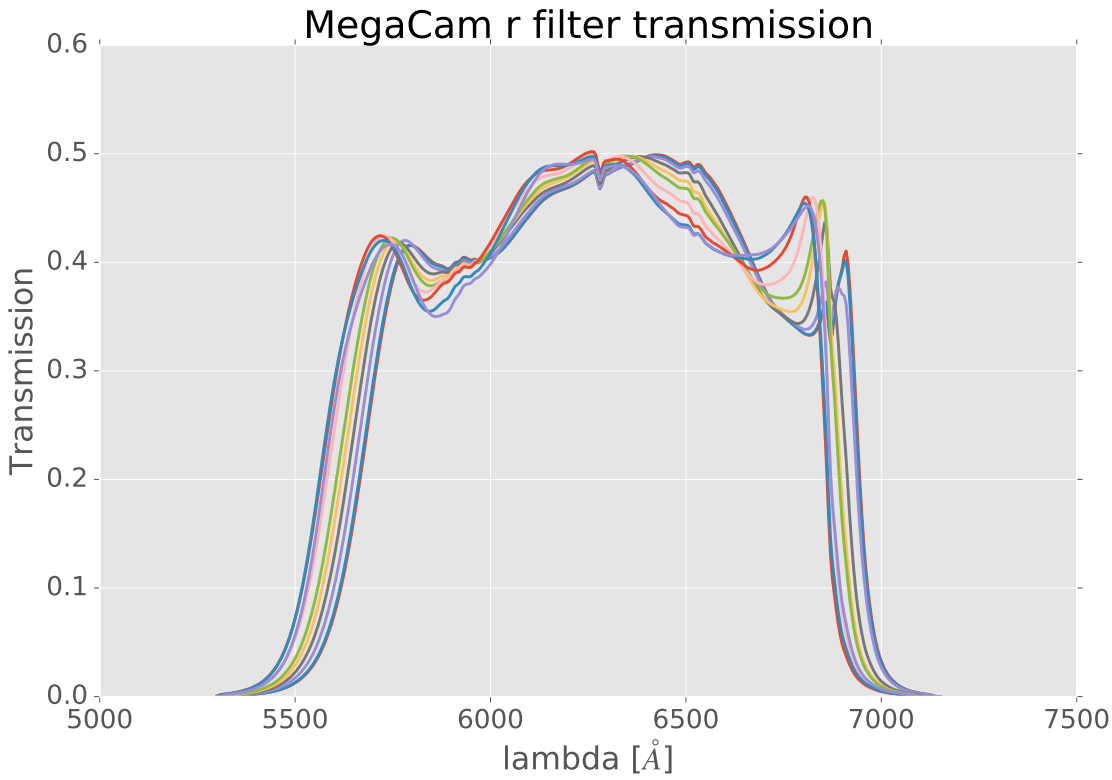

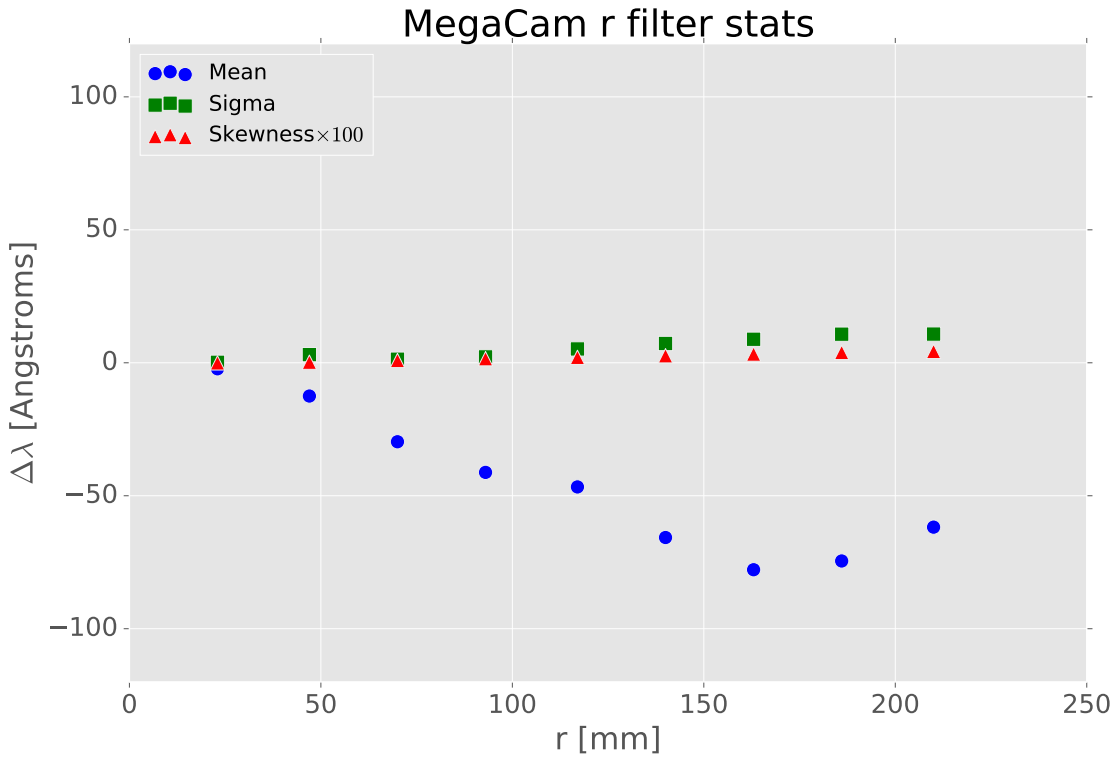

After the decommissioning of the old MegaCam filters, they have been brought to a laboratory in Lyon to be tested with a spectrograph on a measurement bench. The results point out some differences compared to the Betoule et al. study (J.-C. Cuillandre, private communication), but confirm the general trends and orders of magnitude (i.e. typically 80 Angstrom shift from center to border).

Since then, better filters have been obtained and installed on MegaCam. The shift that orignates from manufacturing has been reported to be reduced to 10 Angstroms and the incidence angle shift is a smaller effect than typical variations (figure from Jean-Charles Cuillandre):

[Jean] I am confused by the impact of the incidence angle on the filter. If it's really constant, it's less problematic for photo-z's as the calibration fields will be observed with the same filter. If it varies across the focal plane, it is an effect we need to study. However, since the effect is equivalent to a shift caused by manufacturing, our tests will capture anyway the effect of a shift (due to either effect), which is fine for this study.

4.3.5 The Sloan camera

From Doi et al. (2010).

Filters transmission blue shift: 3 sources to consider

1: blue shift with incidence angle

$$\lambda(\theta) = \lambda_0 \sqrt{1 - (\sin\theta / n_{eff})^2}$$

$\lambda(\theta)$	Blue shifted wavelength
λ_0	Wavelength at normal incidence
θ	Beam incidence max. angle
n_{eff}	Filter effective index (1.5–2.0)

Beam Angle (BA) versus f–ratio + 700nm example:

Imager	*f–ratio*	*f–length*	*FOV*	*BA*	*@700*
LSST	1.2	10.3	3.5	22.1	–16
Blanco–DECam	2.7	11.6	2.2	9.8	–3
JST–JPCAM	3.5	9.1	3.0	8.1	–2
CFHT–MegaCam	4.2	15.1	1.4	6.8	–1
Pan–STARRS	4.4	8.0	3.0	6.5	–1
		m	deg.	deg.	nm→

blue shift considered uniform over the whole FOV

2: blue shift from manufacturing

- Filter maximum radius:

LSST	r=35cm
Blanco–DECam	r=25cm
Pan–STARRS	r=25cm
CFHT–MegaCam	r=20cm
JST–JPCAM	r=12cm

- Current imagers technology:
  Gradual linear shift over FOV vs center:
  Realistic: –1.0 nm shift at r=30cm
  At best: –0.5 nm shift at r=30cm
  At worst: –2.0 nm shift at r=30cm

3: blue shift with temperature

- Faint effect: ~2x10E–2 nm per deg. C.
- Observing sites can see large ranges
- Uniform shift over the whole FOV

Gradual shift and temperature gradient estimates : B. Sassolas, N. Regnault, M. Betoule (IN2P3)

Blue shift in modern filters (from J.-C. Cuillandre)

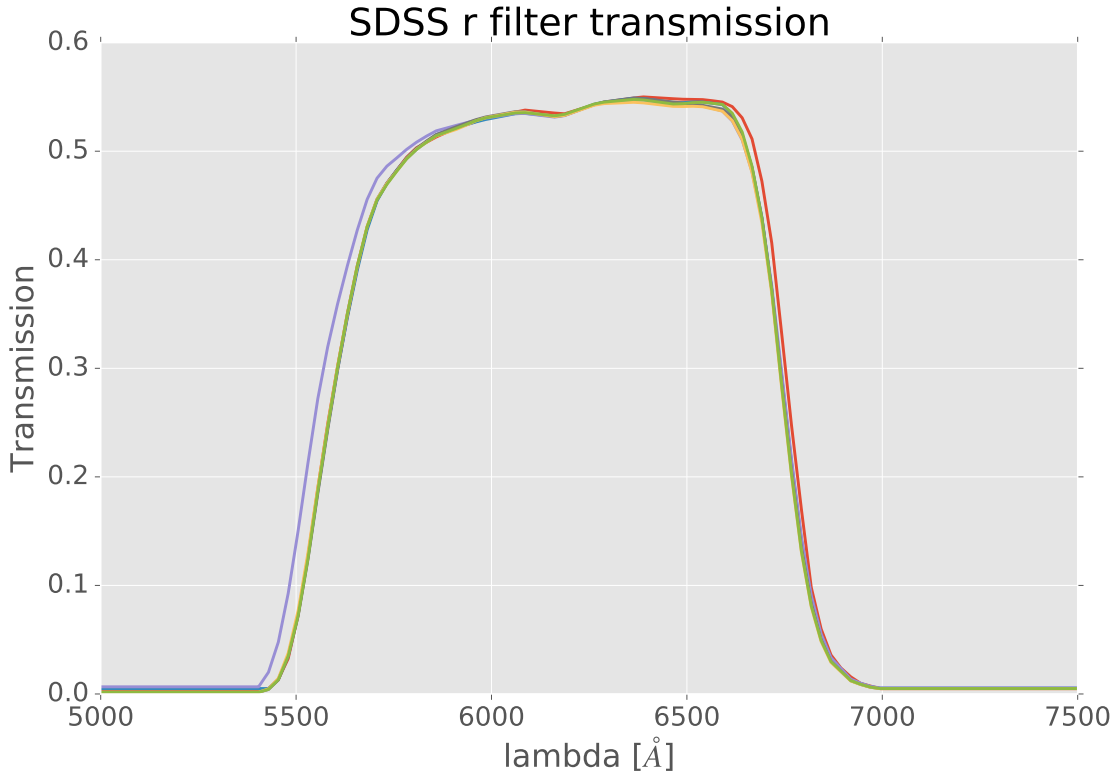

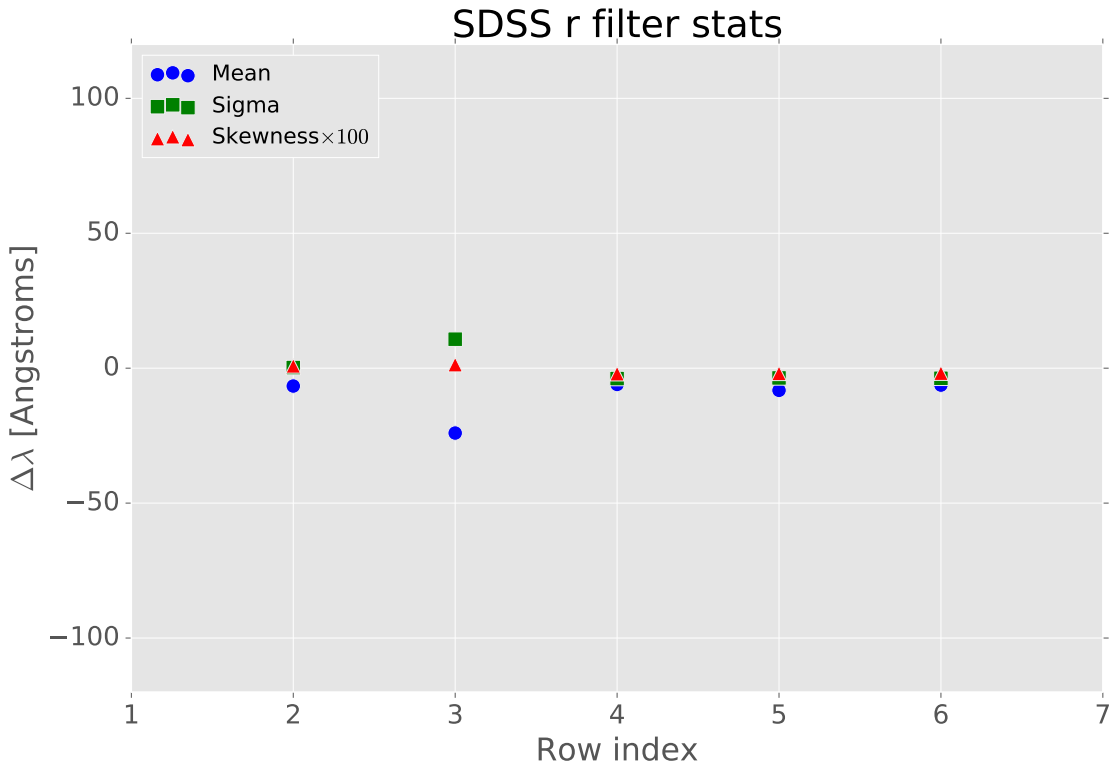

4.3.6 DECam at the Blanco telescope

Burke et al. (2017) Li et al. (2016)

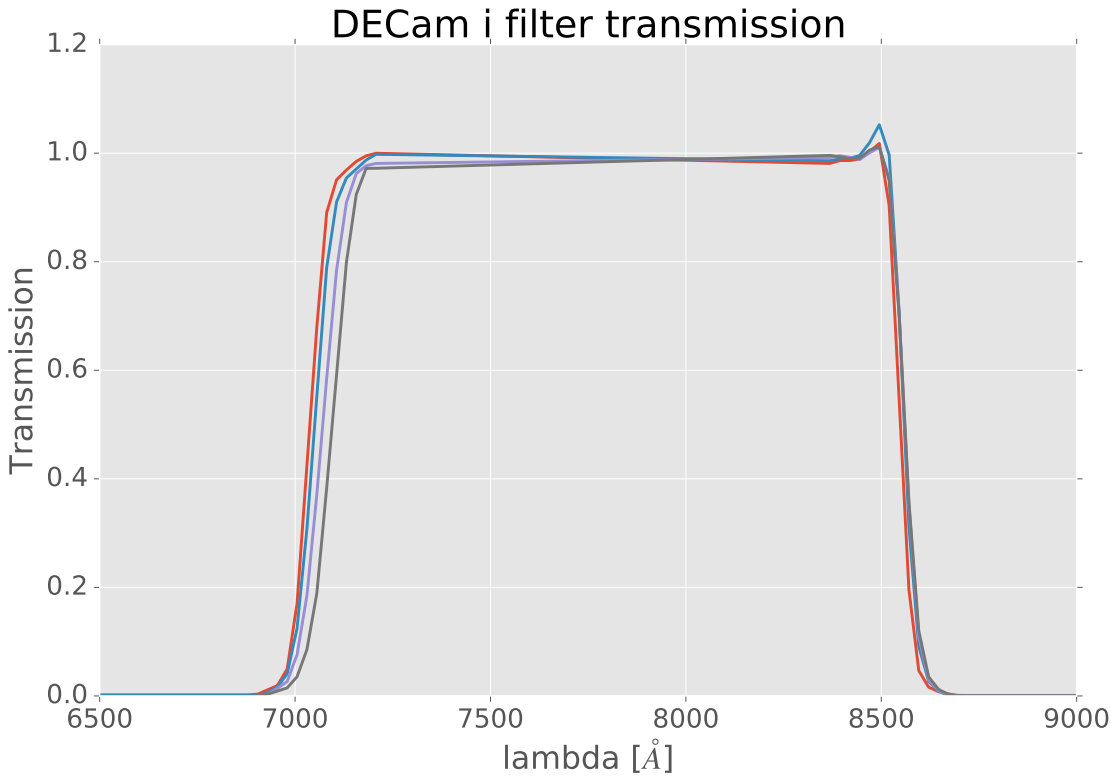
DECam i filter transmission
Transmission
lambda [Å]
1.2
1.0
0.8
0.6
0.4
0.2
0.0
6500
7000
7500
8000
8500
9000

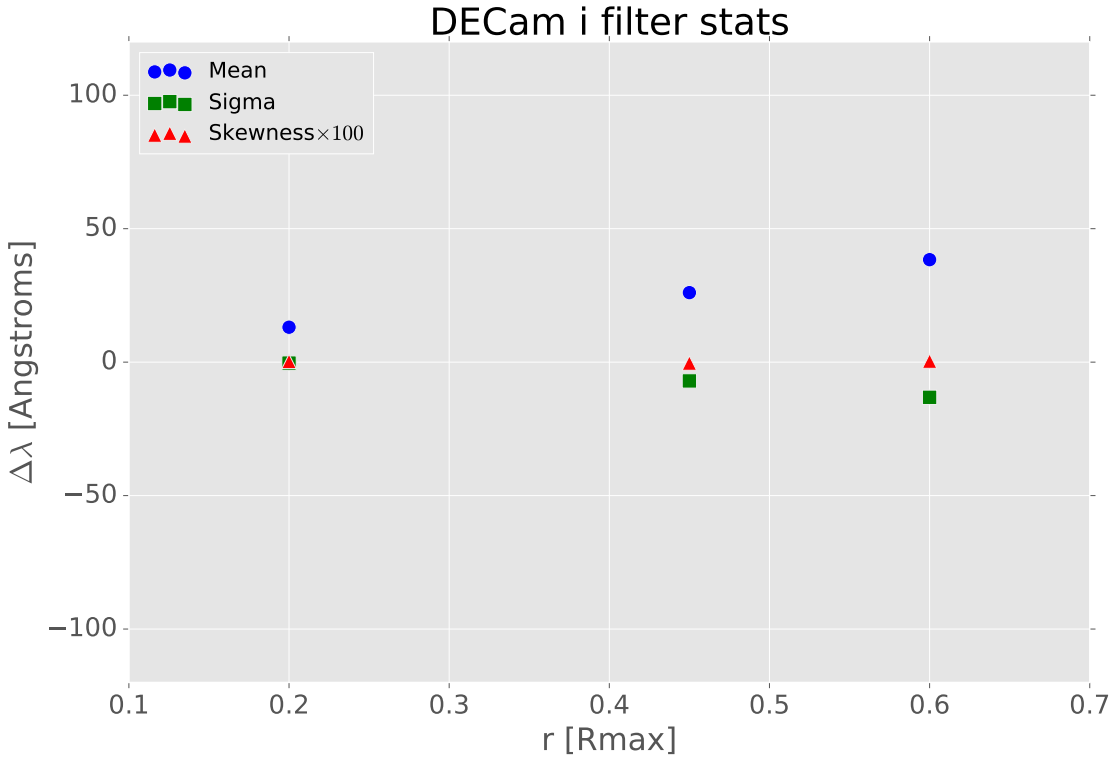
DECam i filter stats
Mean
Sigma
Skewness×100
Δλ [Angstroms]
r [Rmax]
100
50
0
−50
−100
0.1
0.2
0.3
0.4
0.5
0.6
0.7

4.3.7 Hyper Suprime Cam at Subaru

The first *i*-band and *r*-band filters of the Hyper Suprime Cam suffered from an important wavelength shift on the cut-on and cut-off wavelengths in the form of a concentric ring located about half way between the center and the edge. Miyazaki et al. (2017) report a shift of up to 7 nm (70 Angstroms). Since 2016, both filters have been replaced with more uniform transmissions.

4.4 Modeling the variations

We model in this section the typical filter transmission variations and a range of amplitudes. Our approach is to be as close to the reality as possible but with no actual prediction for the typical variations that the Euclid survey will encounter. The goal is to establish a set of possible variations and test the impact on photo-z's. It must be used as a ruler to predict the true impact on Euclid (and the actions to take to address the problem) when the actual variations are known.

Therefore, we will test each effect independently and adopt a range of amplitudes to mimic what's observed in different cases.

Based on the discussions with people involved in several surveys and the results presented above, we propose three separate kinds of variations:

- a shift in wavelength (mostly towards the blue)
- a widening (or shortening) of the transmission width
- and a change in slope as a function of wavelength

In fact the change in overall sensitivity can also induce a shift in color if the calibration is unable to correct for it, but this effect is most probably a second-order effect and we focus primarily on the above three effects.

As the reference transmission, we model a *r*-band filter whose response is a top-hat function between 5600 and 7000 Angstroms centered on $< \lambda >= 6300$ Angstroms. The maximum transmission is 0.8.

4.4.1 Shift

We model the shift by simply shifting the transmission towards the blue and the red from -100 Angstrom to +100 Angstrom. We see below that the only impact on the stats compared to the reference filter is a difference in mean wavelength.

4.4.2 Widening

We study the impact of a change in standard deviation between -15 and +15 Angstroms.

4.4.3 Skewing

We model the skewing of the transmission with a linear function with different slopes whose value at the transmission center is always 0.8. We vary the slope between $-1.e-2 \times 6300 \sim -60^\circ$ and $+1.e-2 \times 6300 \sim 60^\circ$, which seem to reproduce well the change in asymetry seen with MegaCam.

4.4.4 Softening

Finally, we add a fourth kind of variation to take into account the arbitrary combination of transmissions with different shapes. This can typically occur when several exposures are stacked together. In addition to the other effects mentioned above, this will result into a softening of the transmission edges, which we model by changing the slopes of the red and blue edges of the transmission.

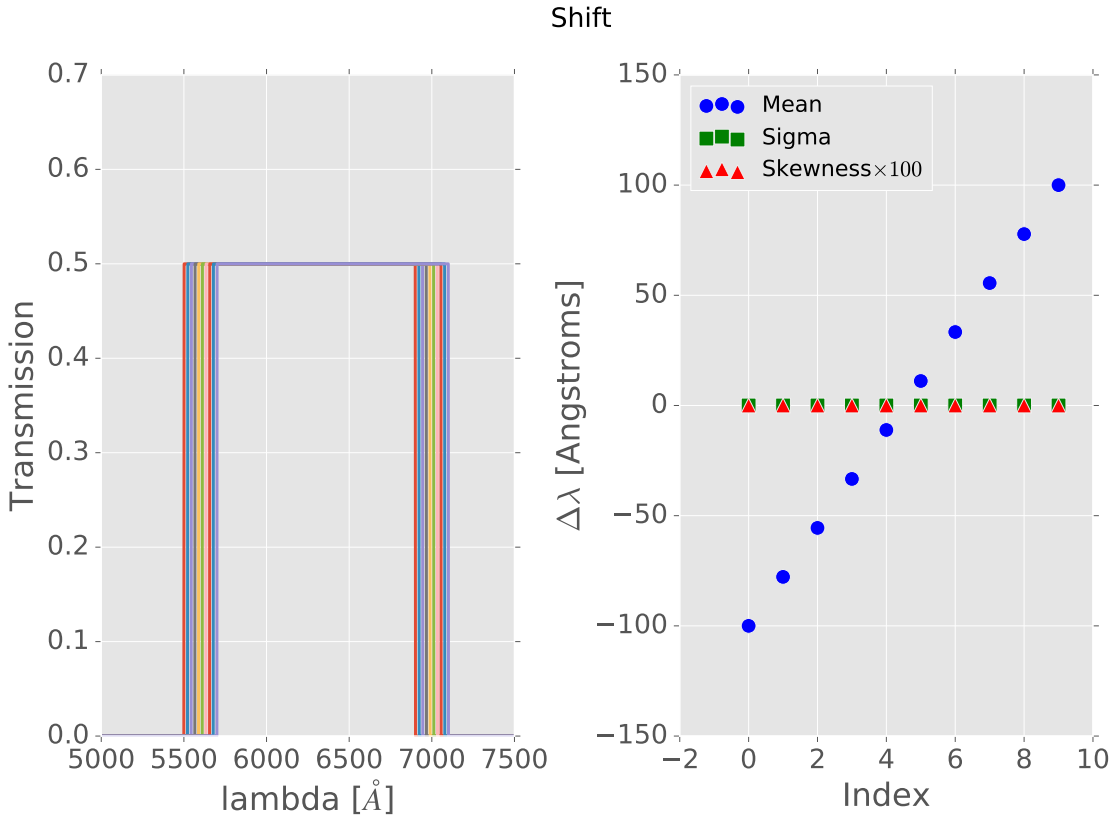
Shift
Transmission
lambda [$\AA$]
$\Delta\lambda$ [Angstroms]
Index
Mean
Sigma
Skewness$\times$100

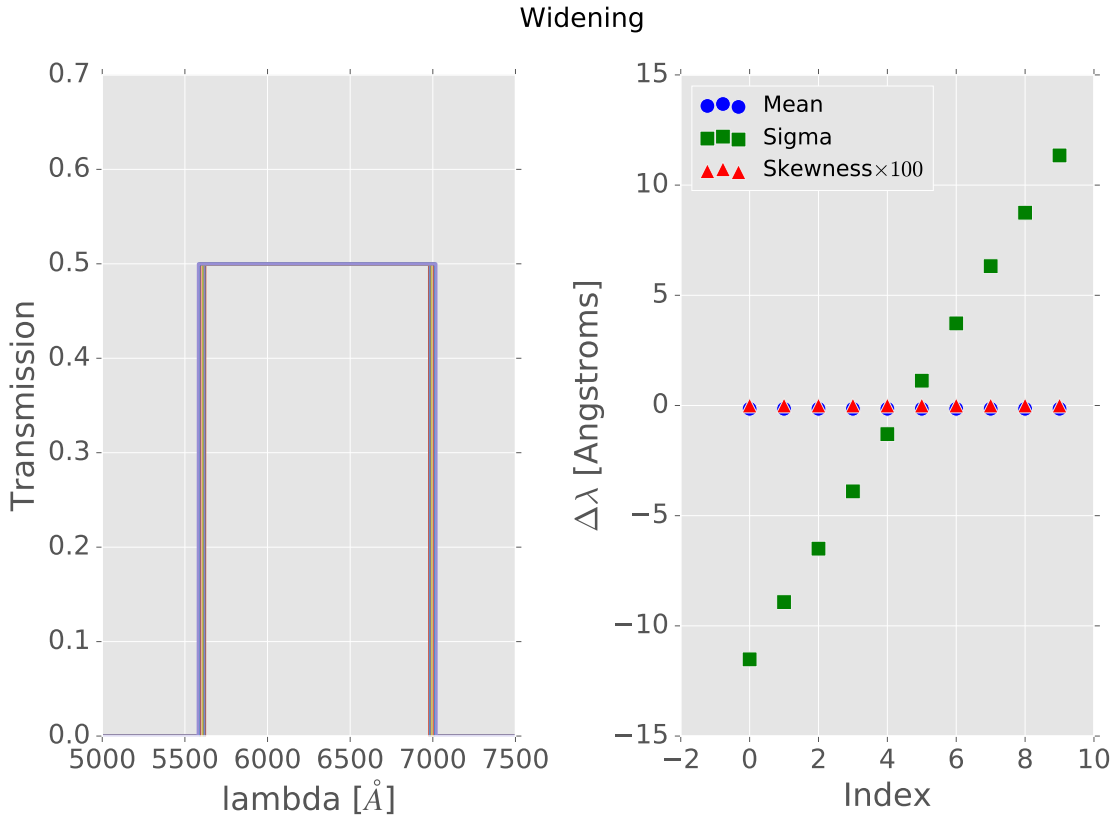
Widening
Transmission
lambda [$\AA$]
$\Delta\lambda$ [Angstroms]
Index
Mean
Sigma
Skewness$\times$100

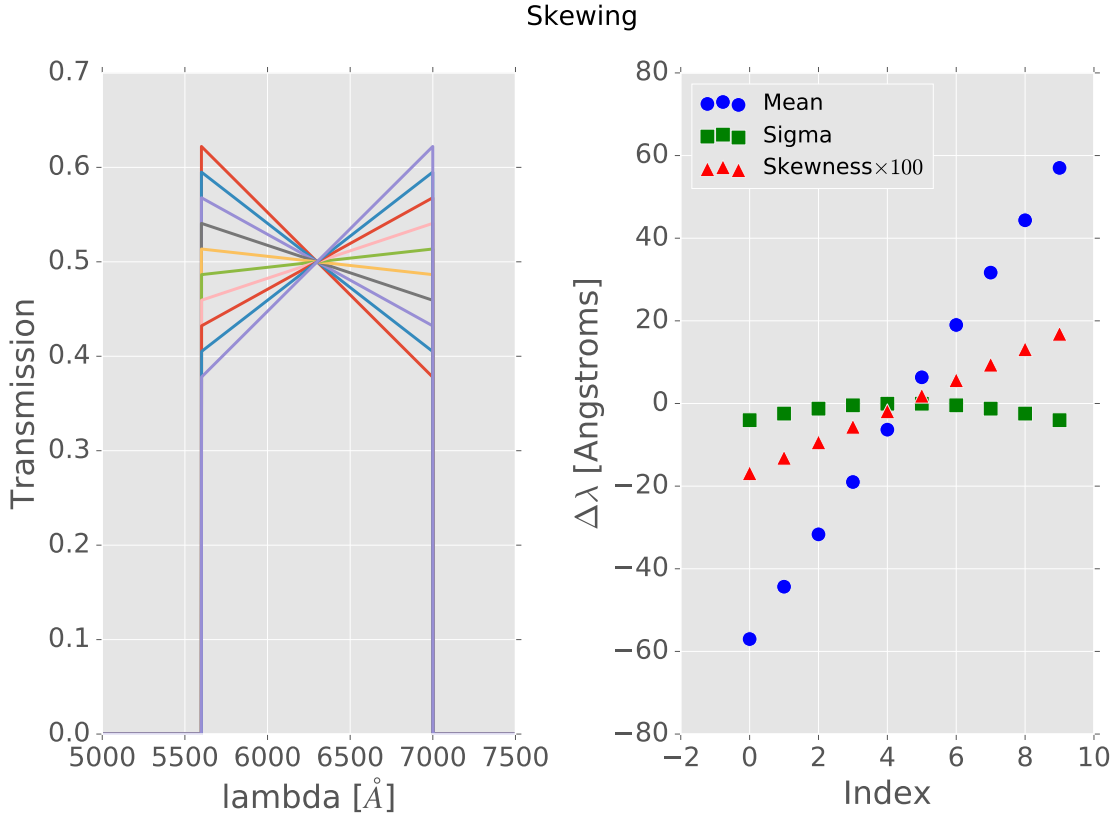
Skewing
Transmission
lambda [Å]
Δλ [Angstroms]
Index
Mean
Sigma
Skewness×100

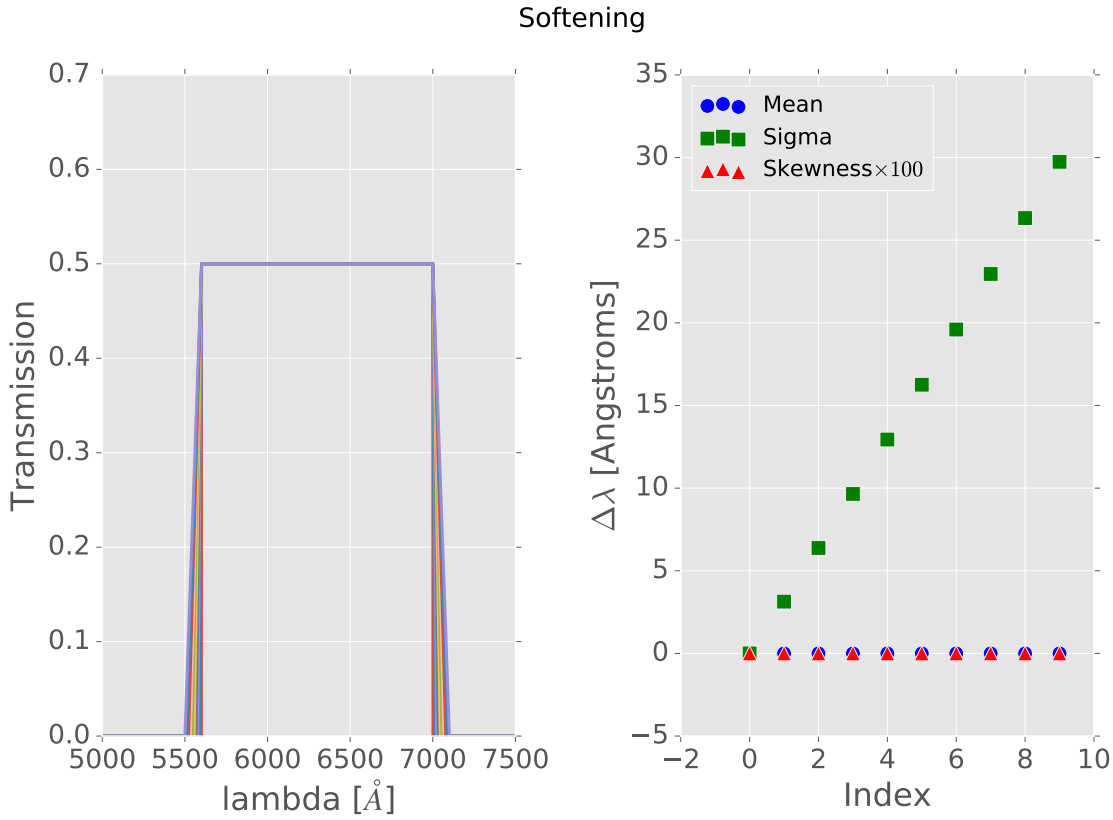

5 Simulations

In this section we perfom the simulations to test the impact of filter varations on photo-z's. The basic principle is to simulate the fluxes with varying transmissions but compute the photo-z's with a reference filter set.

5.1 The reference filter set

The reference filter set is composed of the Euclid-survey filters, i.e. the PLM vis and near-IR filters and the ground-based filters. For the latter we assume MegaCam-type filters, except for the *r*-band filter for which we assume a transmission whose response is a top-hat function between 5600 and 7000 Angstroms centered on =6300 Angstroms, as we adopted in the previous section, with the slight difference that the maximum transmission is 0.5 (as opposed to 0.8), to mimic the attenuation from the atmosphere and the mirror.

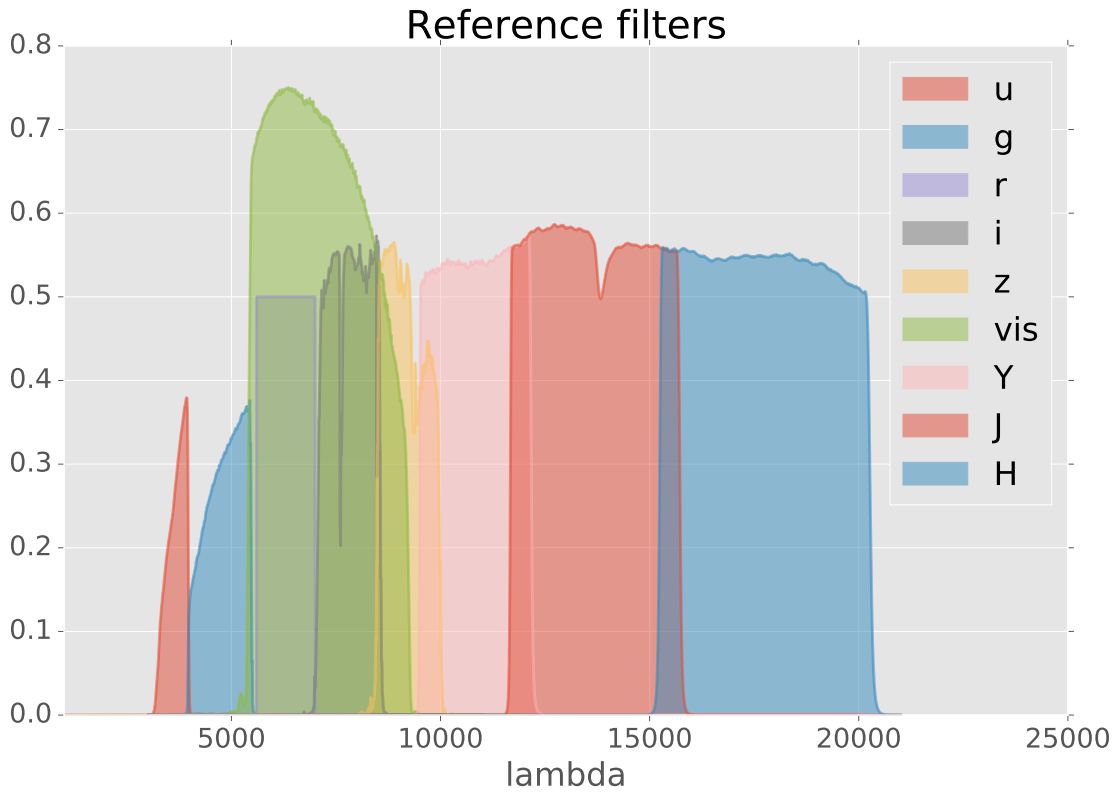

5.2 The variable filter set

We limit ourselves to the variations of the *r*-band filter and focus on the photo-z mean redshift in the interval where the Balmer break goes through the filter wavelength range, i.e between $0.3 < z < 0.8$. We expect that similar trends will occur at different redshifts when other filters are affected by variable transmissions, but we have no reason to think that the effect will be any weaker for the *r*-band than for the other bands, even when accounting for the stretch of the SED with redshift (that could potentielly increase the effect in redder bands), as the performances are always divided by a factor 1+z.

The variations we adopt are identical to those described above and are composed of 10 shifts between -100 and +100 Angstroms, 10 widenings between -20 and +20 Angstroms, 10 angles for the skewing, and 10 softening between 0 and 100 angstroms.

5.3 The simulated sample

We start from real galaxies from the COSMOS field ("COSMOS2015", Laigle et al. 2016) for which a spectral energy distribution (SED) has been fitted to each of them (using the available 30 photometric bands and the best photo-z estimate, Ilbert et al.) and we emulate the galaxies' fluxes in the fixed set of transmissions, as well as the additional 30 variable *r*-band transmission's fluxes.

The main sample is split into two equal samples along a constant RA line to ensure their independence: a deeper calibration sample ("calib") and a target sample ("valid") at the Euclid-Wide depth.

The errors are computed assuming the depth requirements from the Euclid COG group (J.-C. Cuillandre, private communication). Those were also adopted for the photo-z data chalenge 3 (DC3, see documentation). The flux error includes both the Poisson noise from the object brightness and the sky background. The 10-sigmas depths (background-dominated) in optimal apertures ($1.7 * \mathrm{FWHM_{PSF}}^{0.5}$) are given below:

Filter	Depths (10 sigmas)
u	23.6
g	24.5
r	23.9
i	23.6
z	23.4
vis	24.6
Y	23.0
J	23.0
H	23.0

The calibration sample has depths 5 times that of the target catalogue (= 25 times the observing time). Full details are given in the data challenge 3 documentation.

5.4 The simulations

5.4.1 Adopted metric

The photo-z pipeline, developed by the OU-PHZ and the SDC-CH, will proceed in two main steps to compute the photo-z PDFs. The first step consists in producing a PDF for each individual galaxy with the adaquate algorithm to meet the precision requirement (i.e. on photo-z scatter and outlier fraction).

The second step consists in correcting for the mean redshift bias to meet the accuracy requirement, but done for an ensemble of galaxies or directly per redshift bin. In fact several strategies are explored, including a correction per color bin (instead of the full redshift bin), but the result should always be that the mean redshift bias *per bin* must be zero after correction. The operation will most probably be performed using a set of reference spectroscopic redshifts properly weighted to represent the full population, followed by a validation phase involving cluster-z's.

The redshift bins are built using a redshift point estimate extracted from the PDF or (but a simple color selection is also possible), and the mean redshift per bin is computed as the mean of the stacked PDFs.

Our metric to measure the impact of variable filters on photo-z's is the systematic shift $\Delta z_{\rm var}$ affecting the PDF in a given redshift bin, compared to the mean redshift measured when the transmissions are fixed (i.e. when both the calibration and target samples share the exact same filter set):

$$\Delta\langle z\rangle_{\rm var} = \langle z\rangle_{\rm var} - \langle z\rangle_{\rm fix} \tag{5}$$

5.4.2 The photo-z algorithm

We use the NNPZ algorithm to compute the photo-z PDFs (see details in Tanaka et al. 2017, PASJ, psx077, with the exception that here we do not make use of any flux, only colors in the form of magnitude differences), which is the current baseline for the OU-PHZ pipeline. This algorithm has given one of the best performances during the PHZ data challenge 2 and is best mastered by the author of this note, but any other algorithm meeting the requirements on precision could be used without affecting the conclusions of this report.

We extract the median of each PDF as the corresponding point estimate, used for defining the redshift bins and deriving the basic photo-z statistics (scatter and outlier fraction).

5.4.3 Procedure

We first compute the photo-z's using the exact same set of fixed transmissions for both the calibration and target samples. This step serves as a reference for the various photo-z performance statistics.

Secondly, we change the transmission and emulate new fluxes for the target sample. However, we estimate again the photo-z using the identical calibration sample as before, whose fluxes were computed with the fixed set of transmission (i.e. only the fluxes have changed, not the way we compute the photo-z's). This methodology is equivalent to ignoring the variability of the transmissions when computing the photometric

redshifts. For SED fitting method, this would be equivalent to always using the fixed transmissions when computing the flux grid, but applied to galaxies whose fluxes are computed with variable transmissions.

Lastly, we measure the mean redshift per redshift bin, both in the case of fixed transmissions and in the case of variable transmissions. We record the difference between the two and we repeat the procedure for all the different type of variations described above.

6 Results

6.1 Photo-z performances for the fixed transmissions

We first show the photo-z performances in the fixed transmission case (when both calibration and target sample fluxes are computed in the fixed filter set).

6.1.1 Scatter plot

Below is the photo-z ($z_{\rm median}$ estimates) versus the true redshift.

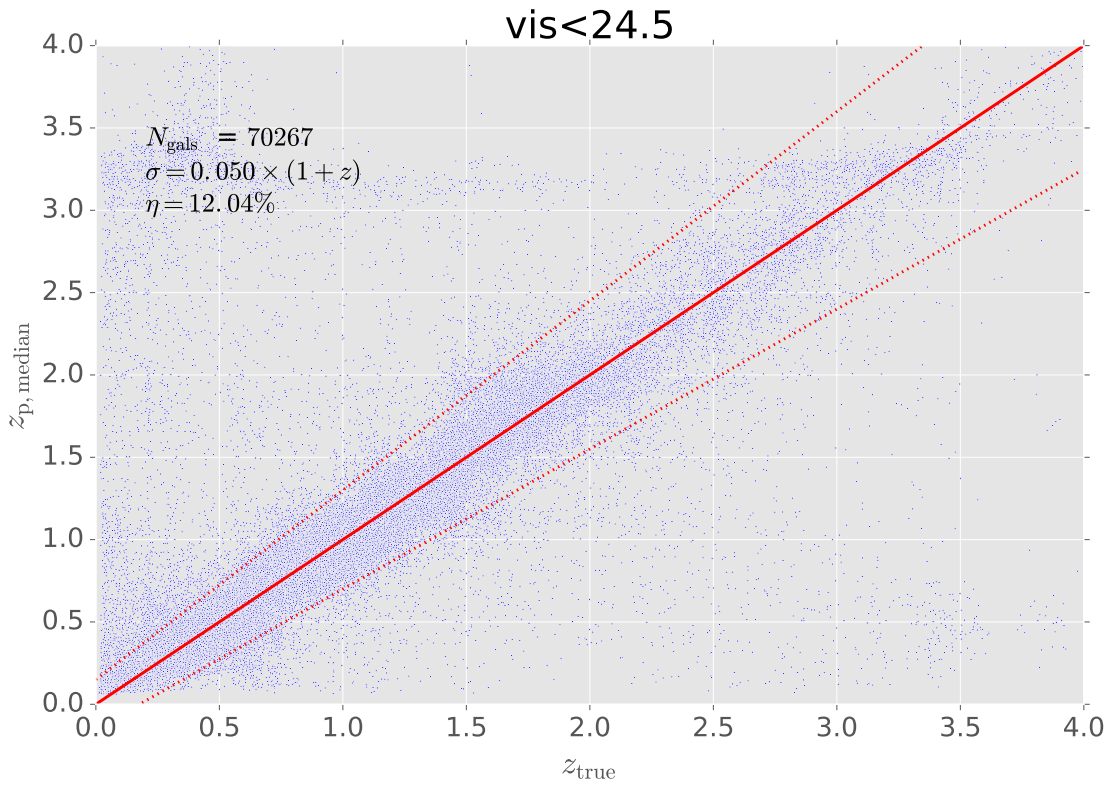

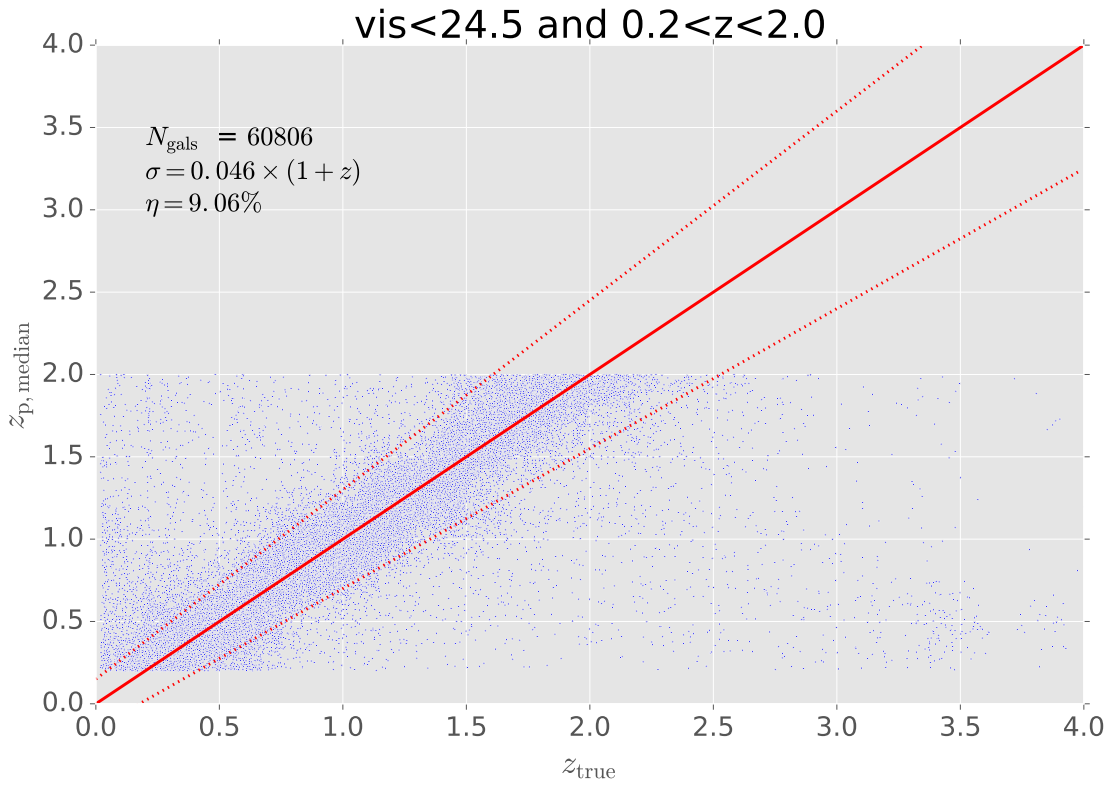

The top figure shows the comparison for the full galaxy sample (i.e. all redshifts) cut at vis$<$ 24.5. The bottom figure shows the comparison with a additional cut in redshift $0.2 < z < 2.0$ corresponding to the limits of the shear sample.

The statistics shown in the figures are computed on the "spec-z" sample (the subset matching the real galaxies having a spec-z) using the weights calculated to represent the full population and given a cut at vis $<$ 24.5, SNR$>$ 10 and $0.2 < z < 2.0$ to match the shear sample. They are expressed for the point estimates (the median redshift of the PDFs) and slightly differ from the metric defined by OU-PHZ which are based on the stacked PDFs. Nevertheless, these statistics suggest the photo-z's meet the requirements ($\sigma < 0.05 \times (1+z)$ and $\eta < 10\%$) and are therefore well suited for our tests.

6.1.2 Mean redshift

In the example below we show the stacked PDFs in the redshift interval $0.5 < z < 0.6$.

Starting from now and for the rest of the note, galaxies are no longer weighted. This is to avoid the dispersion caused by the weighting scheme when splitting per redshift bins. This point will be addressed later, by running the simulations on the full sample.

```
<matplotlib.text.Text at 0x1a0fe4b8d0>
```

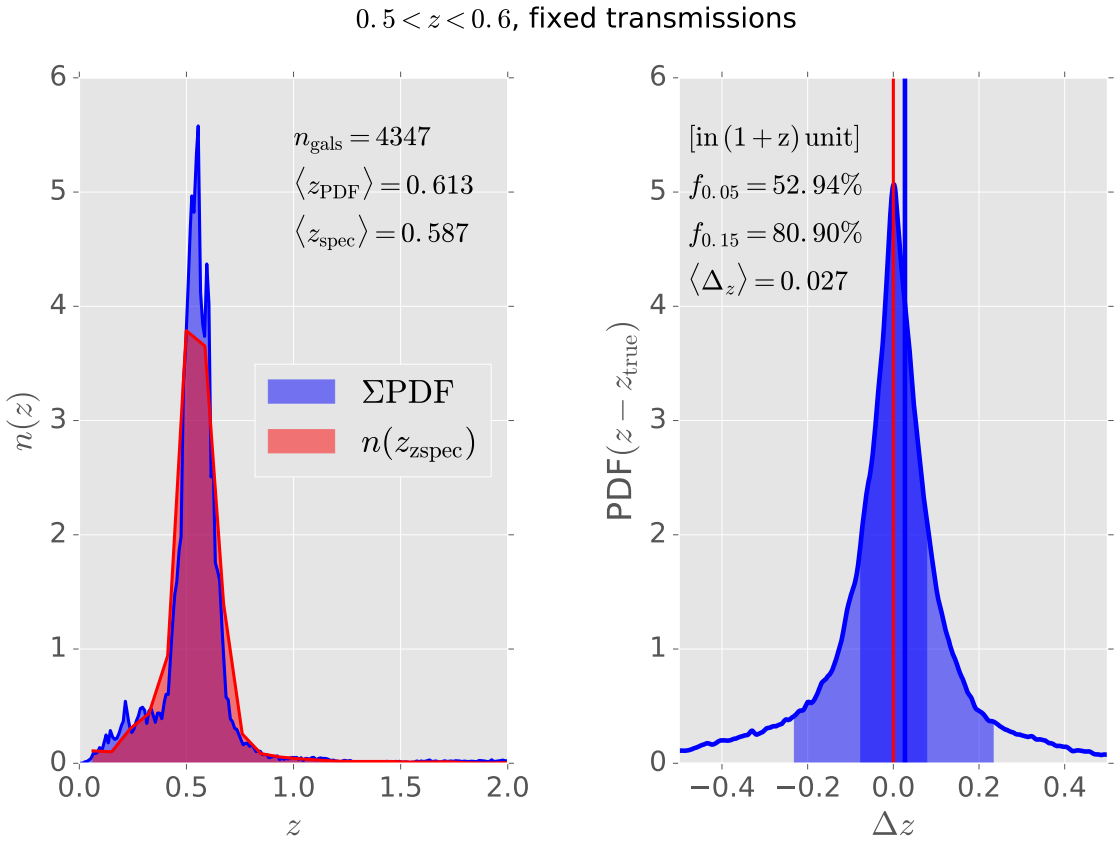

The left-hand plot shows the redshift distribution for the true redhsifts (histogram of the point estimates), in red, and the sum of the estimated PDFs in blue.

The right-hand panel shows the stacked PDF shifted with respect to the true value. The various statistics correspond the metric define by OU-PHZ for measuring the photo-z performances on PDFs.

The mean redshift bias is shown as the Δz value.

6.2 Photo-z performances for the variable transmissions

In this section we compare the fixed-transmission quantities versus those computed with the variable transmissions.

6.2.1 Flux differences

We first show the difference in magnitudes caused by the variable transmissions as a function of redshift. For this we compare the *r*-band fluxes computed in the variable transmissions in the three most extreme cases (shifted by -100 Angstroms, widened by 20 Angstrom and a slope of -0.63), compared to the *r*-band fluxes computed in the fixed transmission.

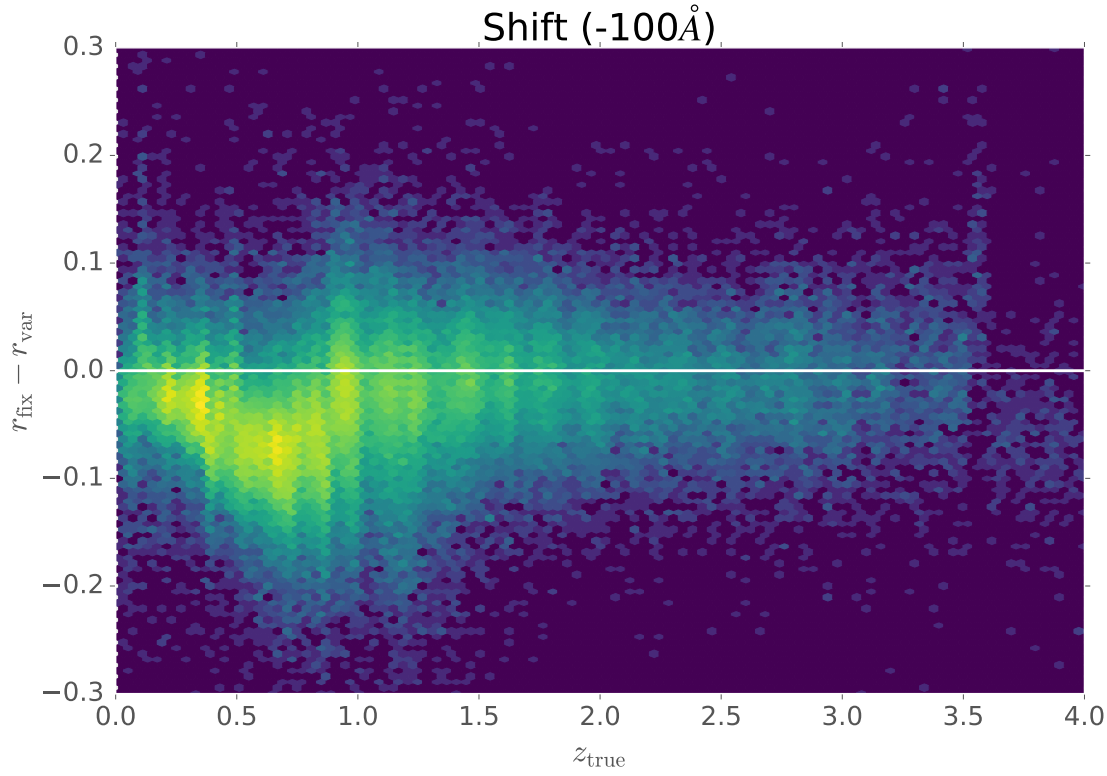
Shift (-100Å)
0.3
0.2
0.1
0.0
−0.1
−0.2
−0.3
$r_{\rm fix} - r_{\rm var}$
0.0
0.5
1.0
1.5
2.0
2.5
3.0
3.5
4.0
$z_{\rm true}$

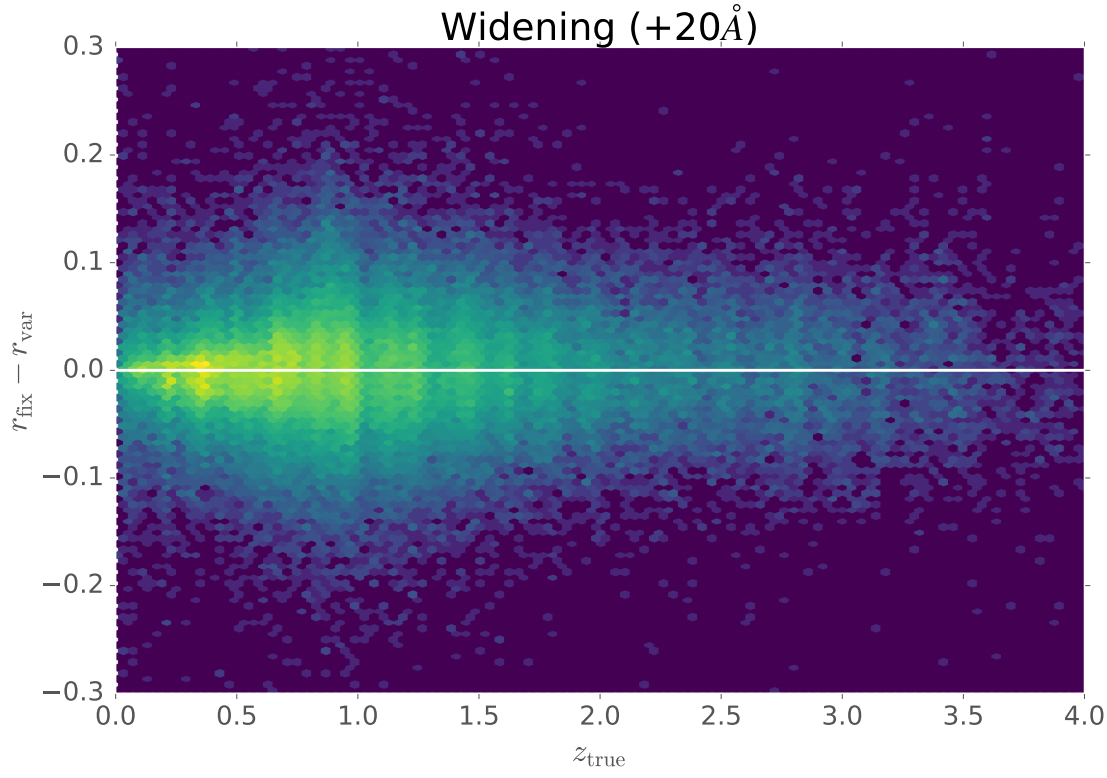
Widening (+20Å)
0.3
0.2
0.1
0.0
−0.1
−0.2
−0.3
$r_{\rm fix} - r_{\rm var}$
0.0
0.5
1.0
1.5
2.0
2.5
3.0
3.5
4.0
$z_{\rm true}$

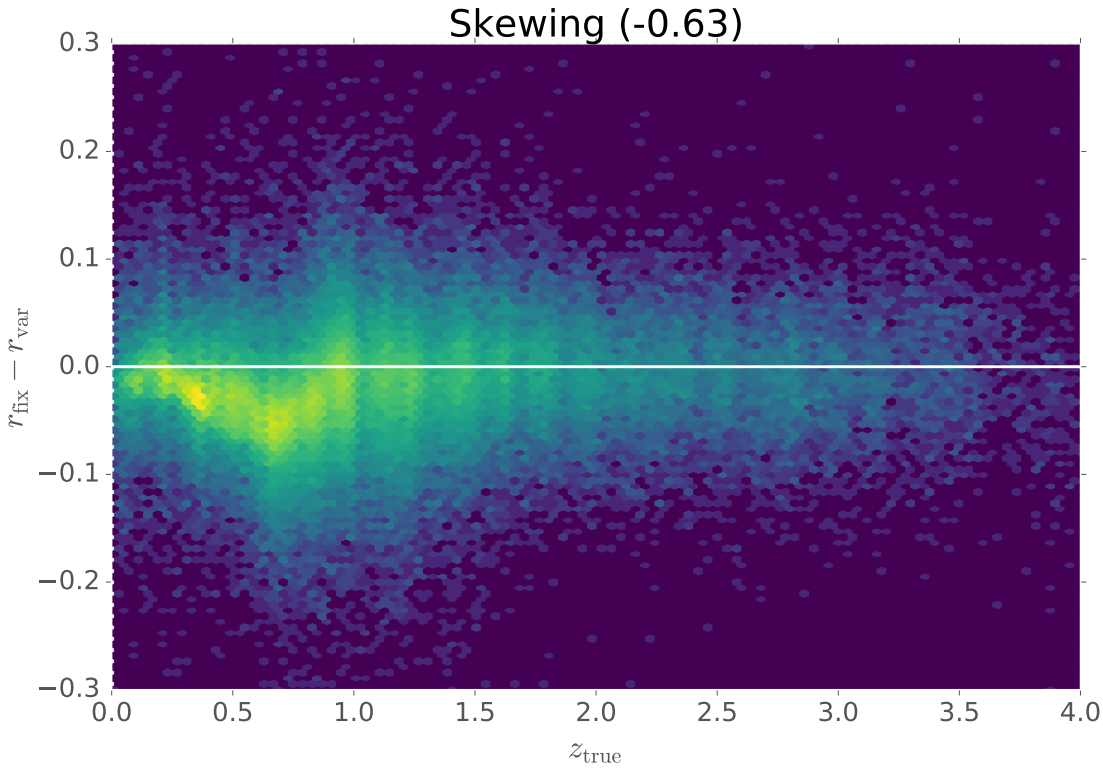
Skewing (-0.63)
0.3
0.2
0.1
0.0
−0.1
−0.2
−0.3
$r_{\rm fix} - r_{\rm var}$
0.0
0.5
1.0
1.5
2.0
2.5
3.0
3.5
4.0
$z_{\rm true}$

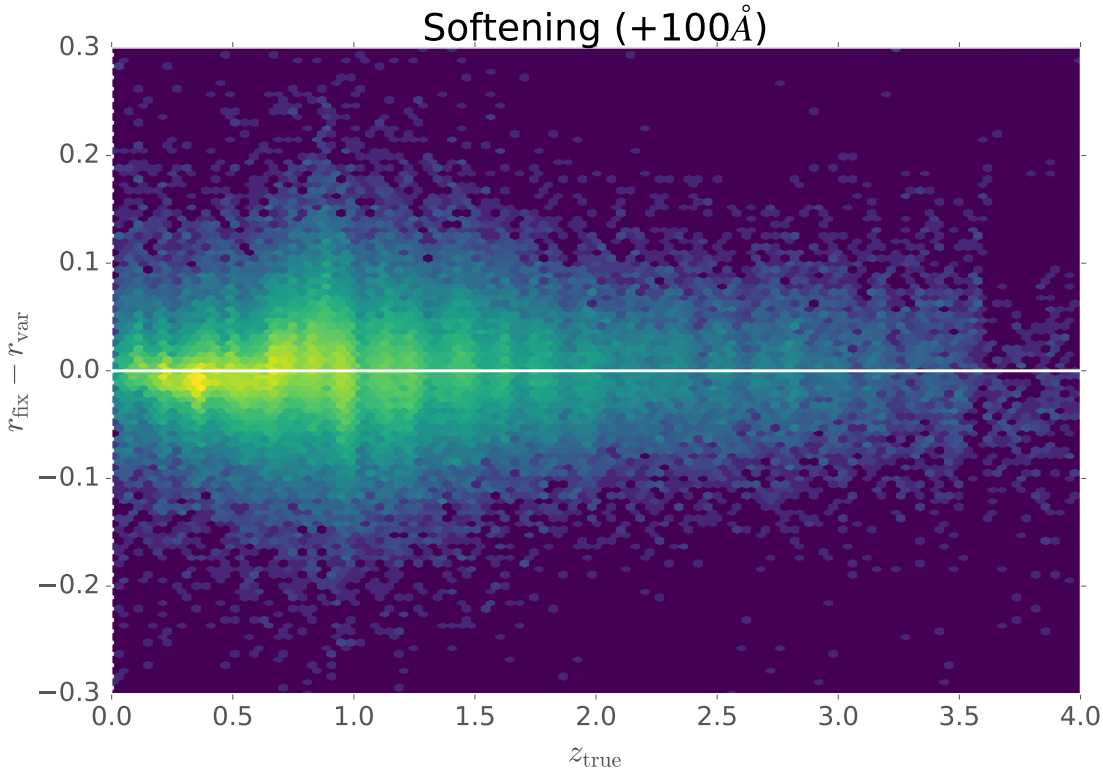
Softening (+100Å)
0.3
0.2
0.1
0.0
−0.1
−0.2
−0.3
$r_{\rm fix} - r_{\rm var}$
0.0
0.5
1.0
1.5
2.0
2.5
3.0
3.5
4.0
$z_{\rm true}$

As expected, we see that the redshift range where the Balmer break goes through the *r*-band, i.e. $0.3 < z < 0.8$, is the most affected. The shift, due to our chosen range (-100 to +100 Angstroms) is the most problematic case, leading up to 0.1 magnitude difference at worst ($z \sim 0.5$). The widening has, on average, almost no impact, but this is also expected since in this experiment we neglect the calibration issues caused by the variable transmissions. The widening will most ptrobably cause, however, addional scattering, but this is barely distinguishable from the statistical scatter in this figure.

Interestingly, the change in slope seems to create a systematic shift similar to the shift in wavelength. This confirms what we saw previously when computing the moments of the transmission: the change in slope is causing a shift of the mean wavelength of the transmission.

6.2.2 Scatter plot

We show the median redshift estimate versus the true redshift for the fixed-transmission case (left) and the variable-transmission case (right), here a shift of -100 Angstroms.

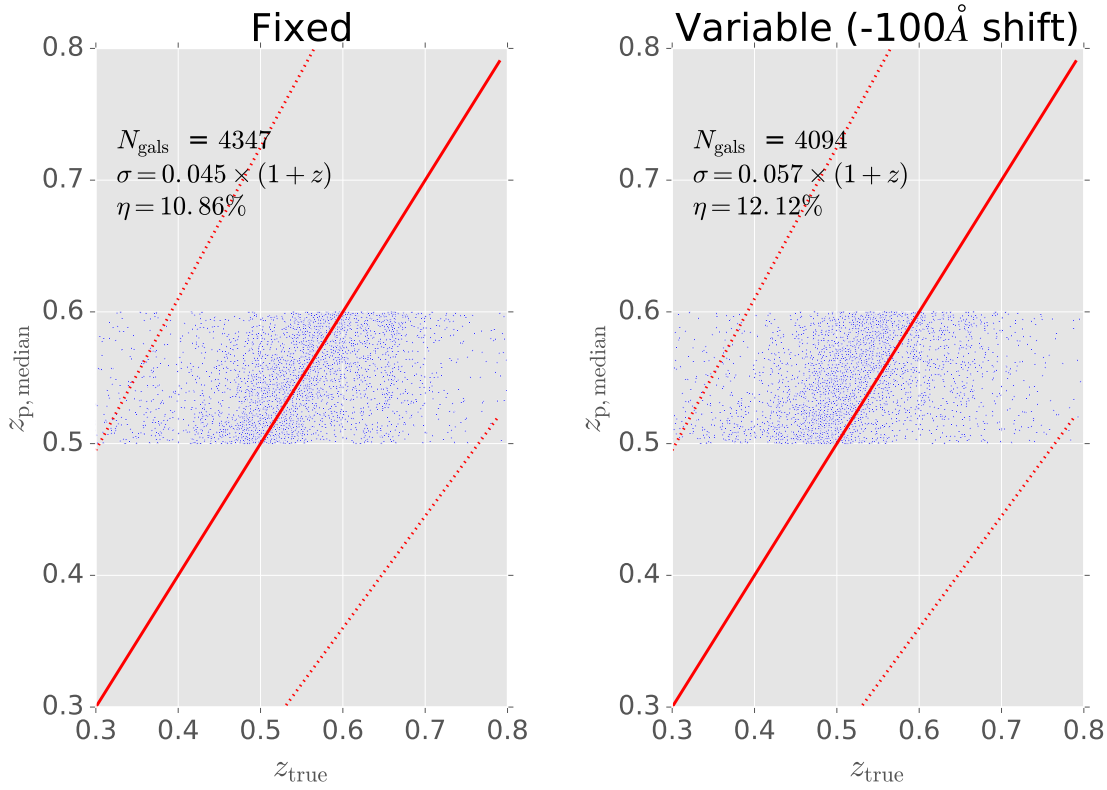

The shift in the transmission causes a systematic shift in the redshift. The target fluxes are affected by a blue shift (-100 Angstroms), causing an artificial red shift of the SEDs, which explains why the true redshift is shifted towards lower values.

6.2.3 Mean redshift

The figure below shows the stacked PDF in the variable transmission case.

```
<matplotlib.text.Text at 0x1a10435910>
```

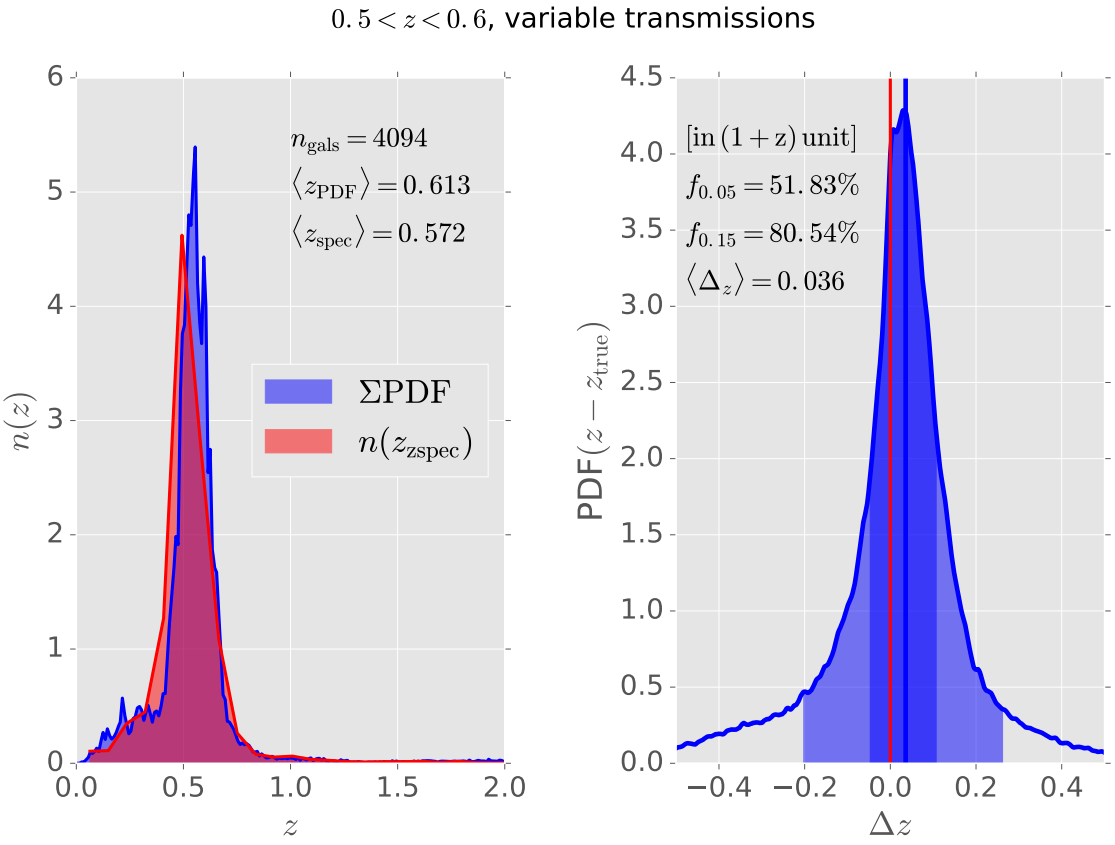

Similarly to the scatter plot, a clear systematic mean redshift shift is seen, both for the redshift distribution and the stacked PDFs.

In the next figures we show $\Delta z_{\rm var}$ as a function of redshift, for the shift, the widening and the skewing of the transmission. In each case we only show the two extreme cases as well as the middle case which corresponds as the smallest variation.

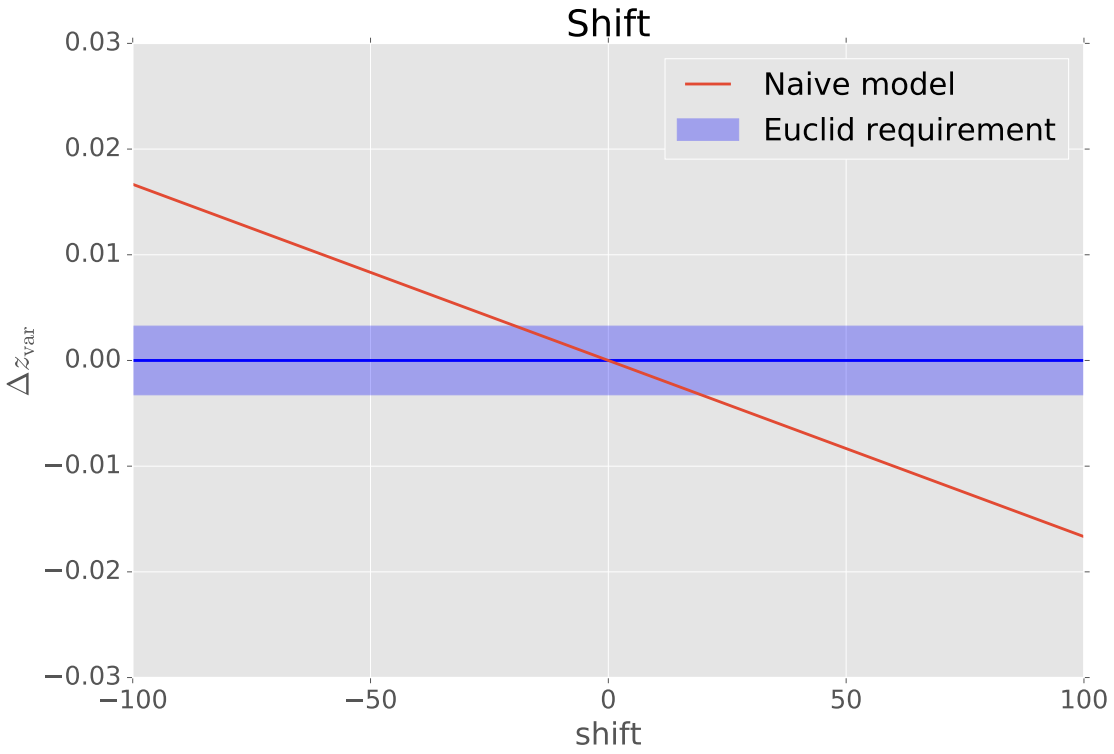
Shift
Naive model
Euclid requirement
0.03
0.02
0.01
0.00
−0.01
−0.02
−0.03
$\Delta z_{\rm var}$
−100
−50
0
50
100
shift

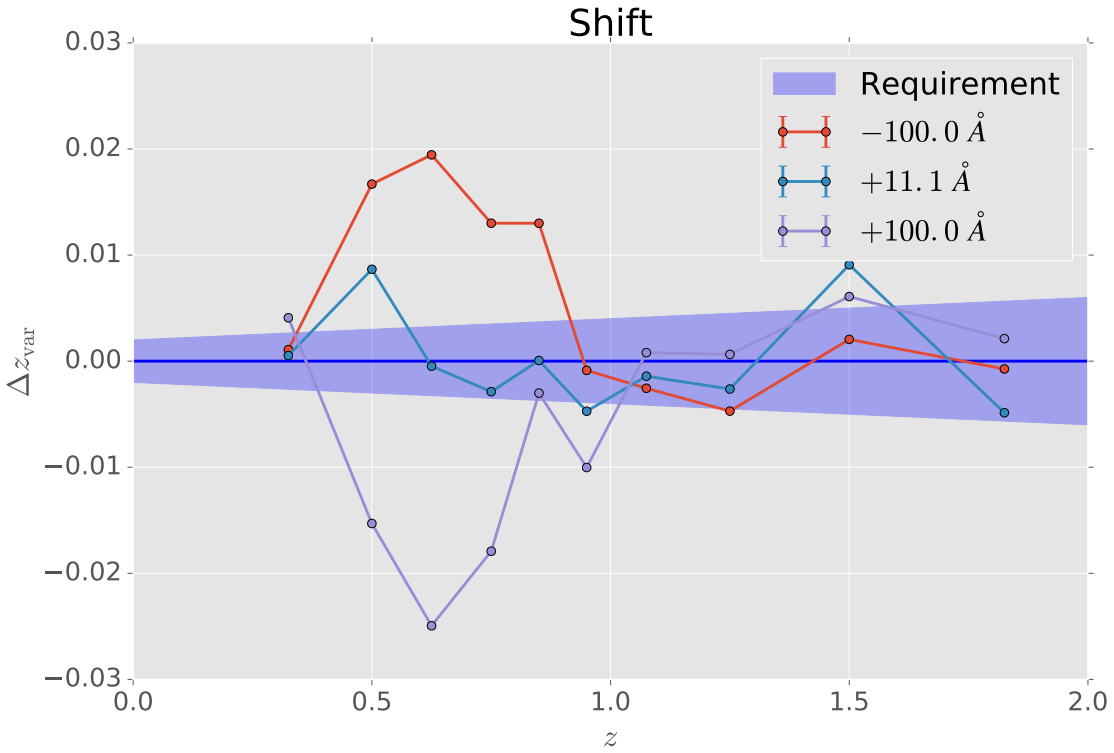
Shift
Requirement
$-100.0\ \AA$
$+11.1\ \AA$
$+100.0\ \AA$
0.03
0.02
0.01
0.00
−0.01
−0.02
−0.03
$\Delta z_{\rm var}$
0.0
0.5
1.0
1.5
2.0
z

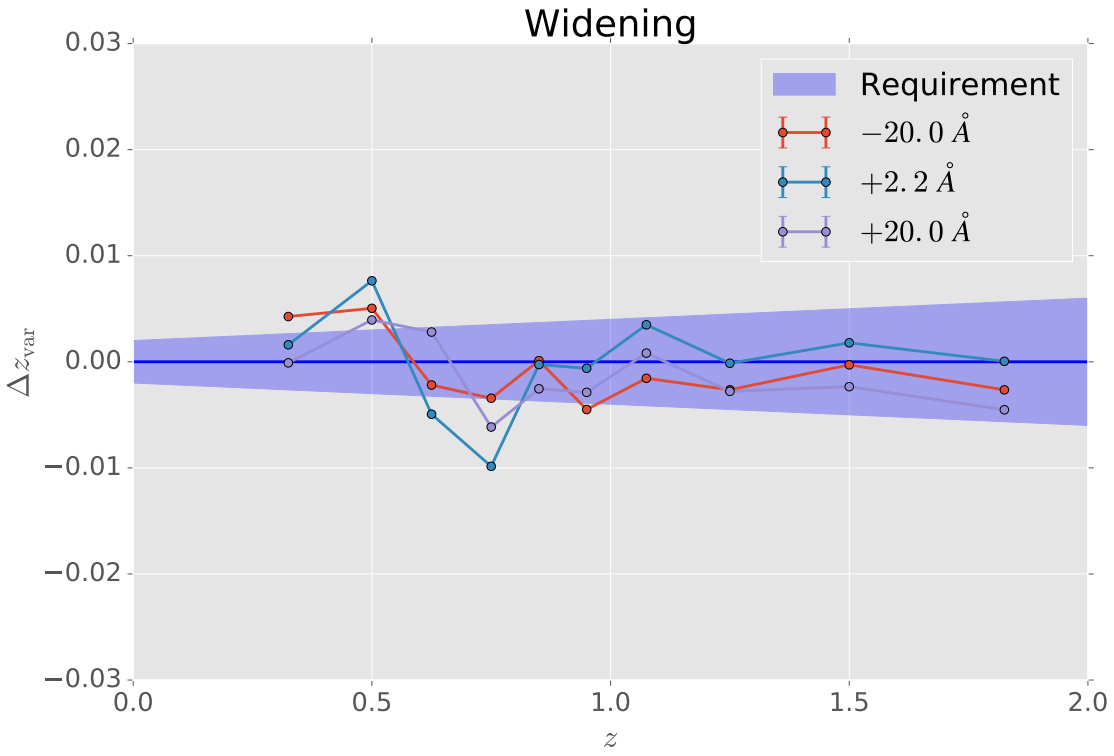
Widening
Requirement
$-20.0\ \AA$
$+2.2\ \AA$
$+20.0\ \AA$
0.03
0.02
0.01
0.00
−0.01
−0.02
−0.03
0.0
0.5
1.0
1.5
2.0
Δz_{var}
z

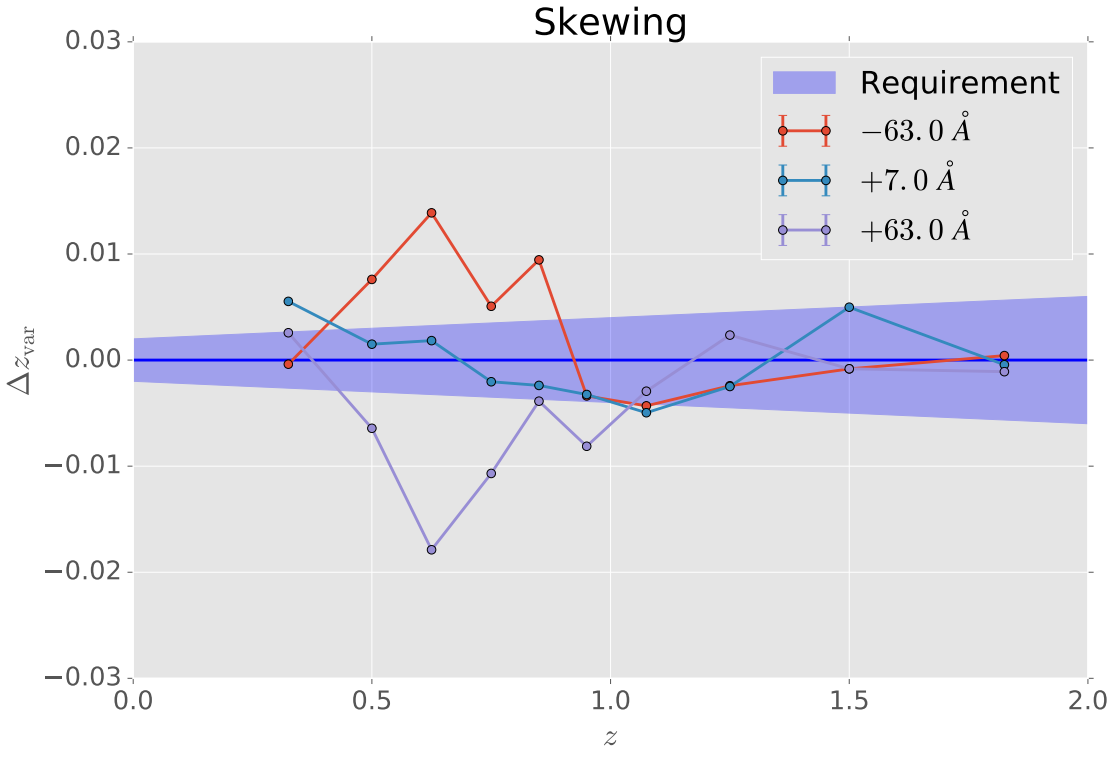
Skewing
Requirement
$-63.0\ \AA$
$+7.0\ \AA$
$+63.0\ \AA$
0.03
0.02
0.01
0.00
−0.01
−0.02
−0.03
0.0
0.5
1.0
1.5
2.0
Δz_{var}
z

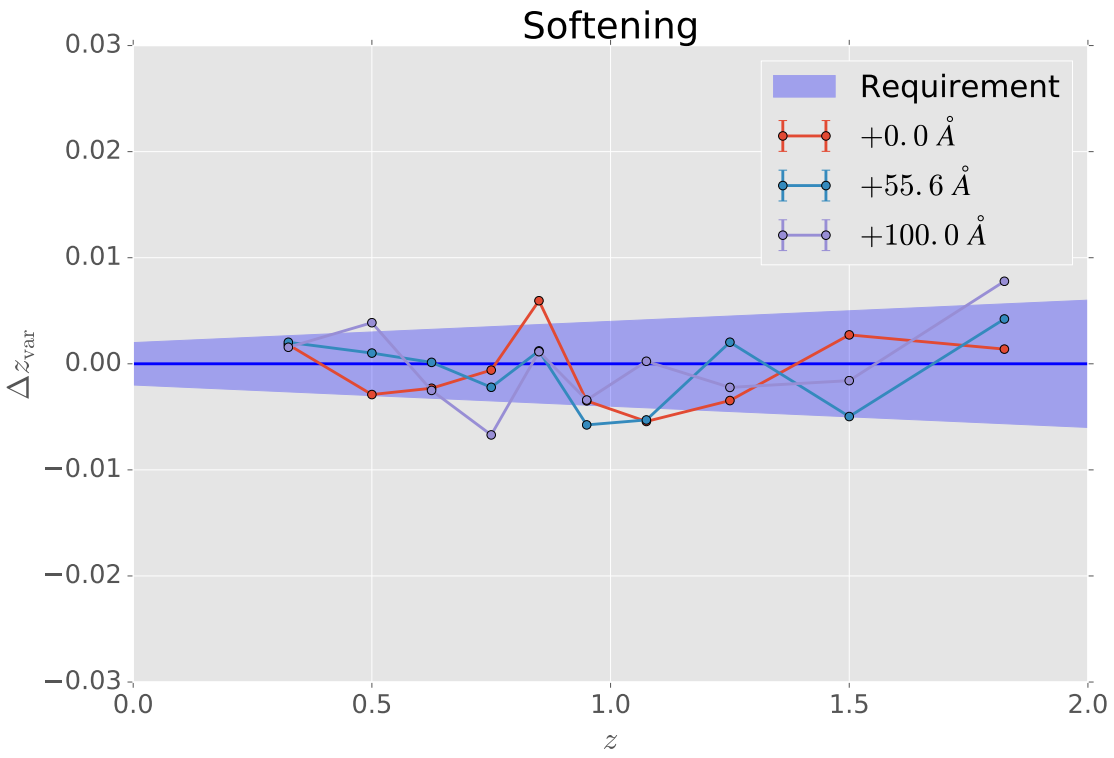

The results above confirm the trends observed in provious sections, and we can already conclude that the shift is the most problematic issue, whereas the impact from widening and the skewing remains lower. As stated above the effect from the skewing shows a similar behaviour as the shift.

Finally we focus on the redshift range that is most impacted, $0.55 < z < 0.7$ and we show $\Delta z_{\rm var}$ as a function of the different simulated variations.

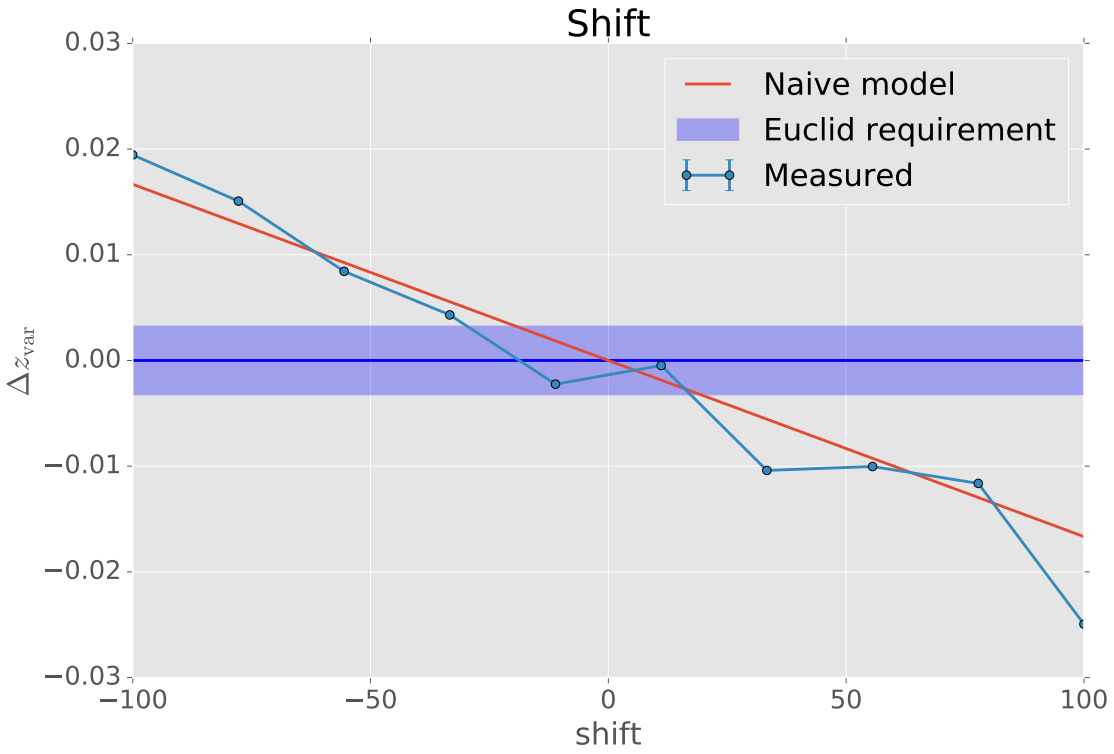
Shift
Naive model
Euclid requirement
Measured
0.03
0.02
0.01
0.00
−0.01
−0.02
−0.03
$\Delta z_{\rm var}$
−100
−50
0
50
100
shift


Widening
Euclid requirement
Measured
0.03
0.02
0.01
0.00
−0.01
−0.02
−0.03
$\Delta z_{\rm var}$
−20
−15
−10
−5
0
5
10
15
20
widening

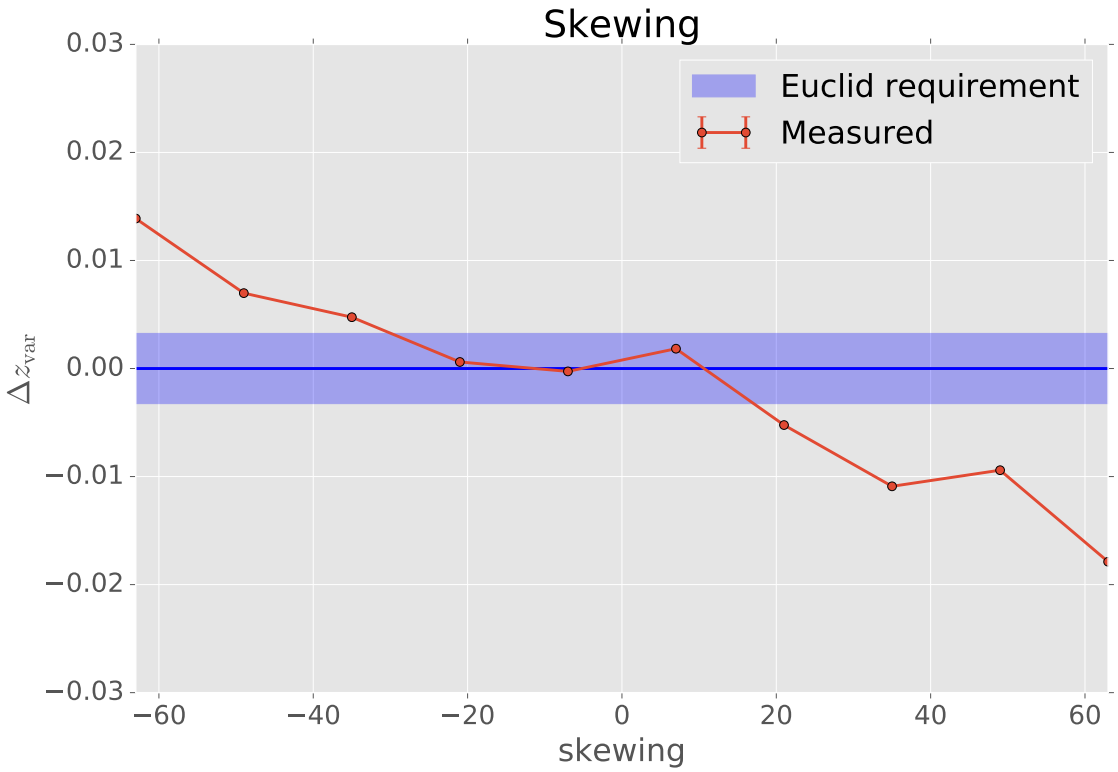
Skewing
Euclid requirement
Measured
0.03
0.02
0.01
0.00
−0.01
−0.02
−0.03
$\Delta z_{\rm var}$
−60
−40
−20
0
20
40
60
skewing

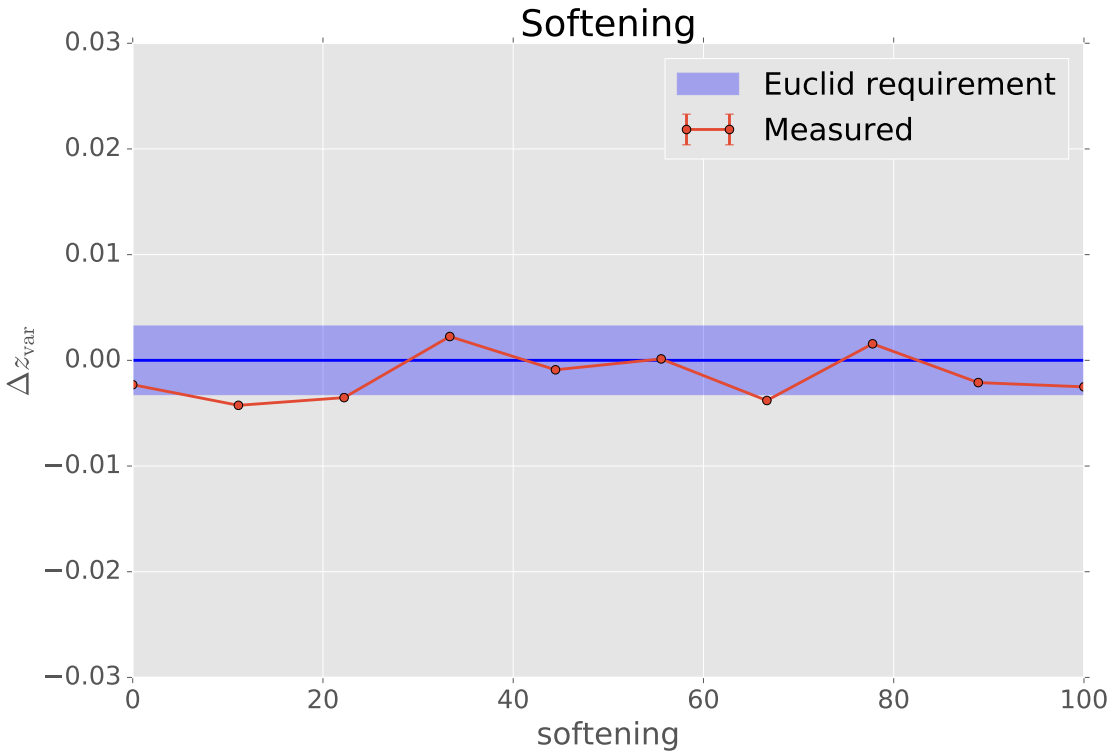
Softening
Euclid requirement
Measured
0.03
0.02
0.01
0.00
−0.01
−0.02
−0.03
$\Delta z_{\rm var}$
0
20
40
60
80
100
softening

The first figure above shows the linear dependence of the redshift bias as a function of the transmission shift. We overplotted the theoretical prediction assuming that the shift can be directly interpreted as an additional redshift on average. The two curves show very similar behaviour which confirms that a shift in wavelength can be directly translated into a redshift bias.

7 Conclusions

We have tested the impact of variable transmissions on photo-z's using simulated fluxes based on the best-fit templates of real galaxies observed with 30 photometric bands in the COSMOS field, and whose emulated fluxes were perturbed according to the minimum-flux SNRs required to meet the precision requirements on photo-z in Euclid.

We only modelled the variations on the *r*-band and we measured the impact in the redshift range which is the most affected, $0.3 < z < 0.8$, due to the predominance of the Balmer break (4000 Angstroms) to constraint the photometric redshift in this interval.

We modeled three main typical variations: a shift in wavelength, a centered widening (or shortening) of the bandpass and a skewing of the transmission, calibrated using real variations measured on various bandpasses and communicated by OU-EXT, the COG, or found in the literature.

The main impact is found to be on the mean redshift of an ensemble of galaxies (the so-called mean redshift bias), and our main findings can be summarized as follow:

- The most problematic effect is a systematic shift in mean redshift and is due to the shift in wavelength of the transmission. The impact on the mean redshift scales linearly with the inverse of the shift in wavelength for the galaxies whose Balmer break is passing through the transmission. For example a typical shift of +40 Angstroms in the *r*-band will cause a mean redshift bias equal to -40/4000.0 = -0.01, i.e. about three times the requirement.
- consequently, a shift as small as 12 Angstrom (1.2 nm) is on the same order as the requirement on the bias
- after calibration, the widening of the transmission has no impact on the mean redshift
- the main effect of the skewing of the transmission is to increase the transmission mean wavelength, hence it has the same affect as a shift of the transmission
- overall the simulations show that the mean wavelength of the filter is the main quantity that impacts the mean redshift for an ensemble of galaxies
- it also means that simply recording the mean wavelength of the transmission and shifting it accordingly seems to be sufficient to correct for the bias

So, it is clear that filter variations impact the mean redshift of large samples of galaxies, even when the variation is small. However, it seems not necessary to propagate the full transmission for each object, but only the mean wavelength of the transmission to correct for the effect.